Ore Geology Reviews 122 (2020) 103500

Contents lists available at ScienceDirect

Ore Geology Reviews

journal homepage: www.elsevier.com/locate/oregeorev

Se minerals in the continental and submarine oxidation zones of the South Urals volcanogenic-hosted massive sulfide deposits: A review

E.V. Belogub[a,*], N.R. Ayupova[a], V.G. Krivovichev[b], K.A. Novoselov[a], I.A. Blinov[a], M.V. Charykova[b]

[a] South Urals Federal Research Center of Mineralogy and Geoecology, Urals Branch of Russian Academy of Sciences, Institute of Mineralogy, Miass 456317, Russia
[b] St. Petersburg State University, Saint-Petersburg, Unversitetskaya nab. 7/9, 199034, Russia

ARTICLE INFO

Keywords:
Selenides
Continental oxidation zone
Submarine oxidation zone
Low-temperature Se thermodynamics
VHMS deposits
Urals

ABSTRACT

The occurrence of Se minerals in continental and submarine oxidation zones of the South Urals volcanogenic-hosted massive sulfide deposits is reviewed. Clausthalite, naumannite and Se-bearing galena occur both in continental and submarine oxidation zones. Native selenium, tiemannite and Se-bearing secondary copper sulfides, sulfosalts and chalcopyrite are found only in the continental oxidation zone, whereas Te-bearing naumannite, bohdanowiczite, and Se-bearing roquesite are identified in the submarine oxidation zone. The Se minerals more often occur in the lower parts of the continental and submarine oxidation zones: secondary copper enrichment subzone and the bottom part of the leaching subzone. In the continental supergene zone, the Se-rich sulfur sand subzone mostly contains Se in forms of native phase and various selenides. Rare Se minerals are found in continental gossans (iron cap) and submarine gossanites (ferruginous products of complete submarine oxidation of massive sulfide ores mixed with hyaloclasts and carbonates). As shown by thermodynamic calculations, presence of selenides in the lower part of the oxidation zone is due to their stability under more oxidizing conditions than the corresponding sulfides at low temperature. The formation of selenides and Se-bearing sulfides in assemblage with Fe(III)-oxyhydroxides can be a result of low activity of reduced S, when Se successfully competes with S for the formation of the chalcogenides. The formation of selenides in the upper part of the oxidation zone is probably related to local redox barrier, which is formed due to vital functions of living organisms. The primary massive sulfide ores with Se-, Pb-, Ag-, and Hg-bearing high-temperature chalcopyrite and another high-temperature primary sulfides, and low-temperature colloform pyrite are source of the selenium and metals for supergene selenides and Se-bearing chalcogenides.

1. Introduction

Mineralogy and behavior of Se under ambient surface conditions are important because of significant biological role of Se and toxic features of its soluble compounds (Holland and Turekian, 2005). Because of the low global mean value of Se ($5{\cdot}10^{-6}$ wt%) and its geochemical affinity to S, Se in the crust mostly occurs as admixture in sulfides however, approximately one hundred Se minerals are known.

The Se minerals are typical of shallow-seated (including epithermal) deposits of volcanic areas (Cook and McPhai, 2001; Jonsson and Wagner, 2002; Ciobanu et al., 2006). Selenides are characteristic of the low- to medium-temperature hydrothermal systems (Brodtkorb and Paar, 1993; Simon et al., 1997; Wagner and Jonsson, 2001). Selenides and native selenium are also described in sedimentary and unconformity-related uranium deposits, where they form under relatively low-temperature conditions (Förster et al., 2005; Krivovichev and Charykova, 2006). Selenides are locally found in the coal-bearing sediments and coal deposits (Finkelman, 1985; Simon and Essene, 1996; Zhu et al., 2012), as well as in phosphate resources sedimentary area (Ryser et al., 2005). In contrast, selenites occur in supergene zones of sulfide deposits and volcanic hydrothermal systems and fumaroles (Krivovichev and Charykova, 2006; Krivovichev et al., 2017).

Selenium in volcanogenic-hosted massive sulfide (VHMS) deposits is an important by-product of massive sulfide processing however, the information on its distribution and Se minerals in the VHMS deposits is still limited (Yushko-Zakharova et al., 1978; Willgallis et al., 1990; Huston et al., 1995; Hannington et al., 1999; Layton-Matthews et al., 2013; Ayupova et al., 2017a; Vikentyev et al., 2019). It is known that Se distribution in sulfide ores of VHMS deposits is uneven. The average Se content of ores from the Urals VHMS deposits varies from 16 to 76 ppm,

* Corresponding author.
E-mail address: belogub_e@yahoo.com (E.V. Belogub).

https://doi.org/10.1016/j.oregeorev.2020.103500
Received 9 September 2019; Received in revised form 15 March 2020; Accepted 25 March 2020
Available online 29 March 2020

depending on the mineral composition and reaches 600 ppm (Vikentyev et al., 2019). The highest Se contents of 3834 ppm have been determined by LA ICP MS for the high-temperature chalcopyrite incrustation of the inner wall of the paleohydrothermal smoker chimney from the ores of the Uralian-type deposits (Maslennikov et al., 2014). In spite of high Se contents, Se minerals have not been found yet in the paleosmoker chimneys, but few selenides have been reported in primary massive sulfide ores of Uralian VHMS deposits: minerals of the galena–clausthalite series in the Cyprus-type Letnee deposit, Dombarovka ore district (unpublished report of Poluektov et al., 1974) and some Uralian-type deposits in the Uchaly ore district (Vikentyev et al., 2019). Berzelianite Cu_2Se and crookesite $Cu_7(Tl,Ag)Se_4$ are found in the Bakr-Uzyak, Yulaly, and Tubinskoe deposits (Kuroko-type) the Baymak ore region (Yushkin, 1991). Kawazulite was identified in the Uralian-type Molodezhnoye deposit of the Uzelga ore district (Vikentyev et al., 2019).

In contrast to primary massive sulfide ores, the spectrum of Se minerals is much wider in the continental oxidation zone of the South Urals VHMS deposits. Native selenium, Fe, Ag, Pb, and Hg selenides and Se sulfosalts, were identified in the lower part of the continental oxidation zone of the Kul-Yurt-Tau (Paley, 1957), Gai (Zaykov and Sergeev, 1993), Dzhusa, Zapadno-Ozernoe, Kontrol'noe (Belogub et al., 2003, 2008), Kaban-I (Blinov and Butnyakov, 2016), Amur (Blinov, 2015), and Yubileynoe (Vishnevsky et al., 2018) deposits. Recently, clausthalite PbSe, Se-bearing galena Pb(S,Se), naumannite Ag_2Se, Te-bearing naumannite $Ag_2(Se,Te)$, bohdanowiczite $AgBiSe_2$, and Se-bearing roquesite $CuIn(S,Se)_2$ were found in assemblage with hematite or magnetite, which are the products of submarine oxidation of massive sulfide ores of the South Urals deposits (Ayupova et al., 2015, 2017a).

It is well known that the oxidation zone forms above ore deposits as a result of the decomposition of primary minerals under influence of surface water and atmosphere and the achievement of new mineral equilibria. These processes can occur both on seafloor and during subaerial exposure. The formation of submarine gossans as a result of decomposition of sulfide minerals during interaction of sulfides with ambient seawater is described in detail at the modern submarine hydrothermal sulfide mounds (Hannington et al., 1988, 1991; Herzig et al., 1991). The Fe-oxide-rich lithified rocks at the top and flanks of massive sulfide ore bodies of the Urals VHMS deposits, similar with modern submarine gossans, were termed "gossanites" (Maslennikov et al., 2012) to discriminate them from continental gossans. The formation of these rocks has been attributed to halmyrolysis (seafloor weathering) of clastic sulfide sediments or plume of settled sulfide particles, which were mixed with background sediments (Maslennikov et al., 2012).

The continental oxidation zone of the South Urals VHMS deposits can broadly be subdivided into several subzones (top to bottom): (1) an iron cap subzone (gossans), (2) a jarosite subzone, (3) a leaching subzone (sands), (4) a native sulfur subzone, and (5) a cementation subzone (subzone of secondary copper sulfide enrichment). Locally, a sooty sand layer, composed of secondary chalcogenides, forms at the lower part of the leaching subzone (Belogub et al., 2008). The thickness, structure, and composition of the individual subzones in fully-developed oxidation zones of the Urals VHMS deposits are highly variable (from few centimeters up to dozen meters). At present, selenides have been found in all subzones, excluding the jarosite subzone (Belogub et al., 2008; Vishnevsky et al., 2018).

A basic profile of the submarine oxidation zone includes (top to bottom): (1) a hematite (oxidation) subzone with clay minerals or chlorite, quartz, and carbonates, (2) a leaching subzone, dominated by barite, pyrite and/or quartz and (3) a supergene enrichment subzone with abundant authigenic chalcopyrite, tennantite, galena, sphalerite and bornite. The thickness of individual subzones varies from few millimeters to 30–40 cm (Maslennikov et al., 2012). Selenides have been found in subzones 1 and 3.

In this paper, we review the accumulation of Se in form of Se minerals in the low-temperature mineral assemblages, which formed during continental and submarine oxidation of sulfide ores of the South Urals VHMS deposits, and discuss their formation conditions.

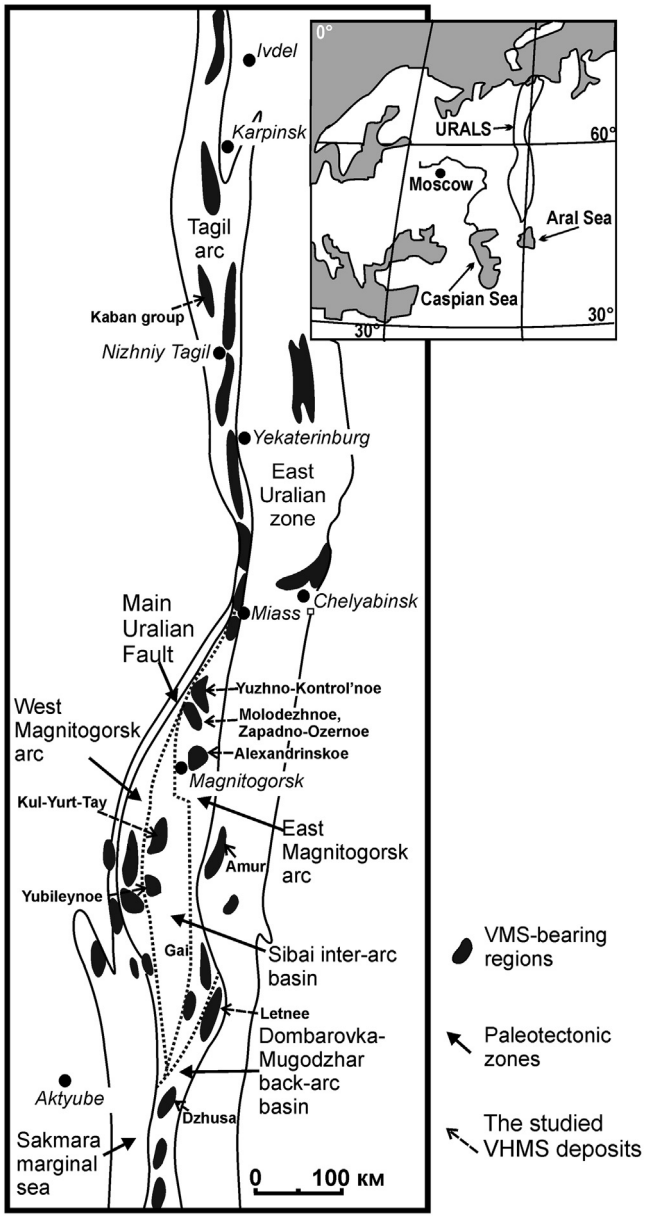

Fig. 1. VHMS-bearing regions of the Urals and position of the deposits with surface or submarine oxidation zones, containing identified selenium minerals (based on Prokin and Buslaev, 1999; Zaykov et al., 2001; Herrington et al., 2005).

2. Analytical methods

Samples for this study were collected from the Yubileynoe, Zapadno-Ozernoe and Molodezhnoe VHMS deposits, as well as from Amur Zn deposit (Fig. 1). For comparison, we will briefly review the findings of Se-bearing minerals in the continental oxidation zones of the South Urals Kul-Yurt-Tau, Gai, Kaban-I, and Dzhusa deposits and submarine oxidation zone of the Aleksandrinskoe deposit. All analytical works were carried out at the Institute of Mineralogy of Russian academy of science, Miass, Russia.

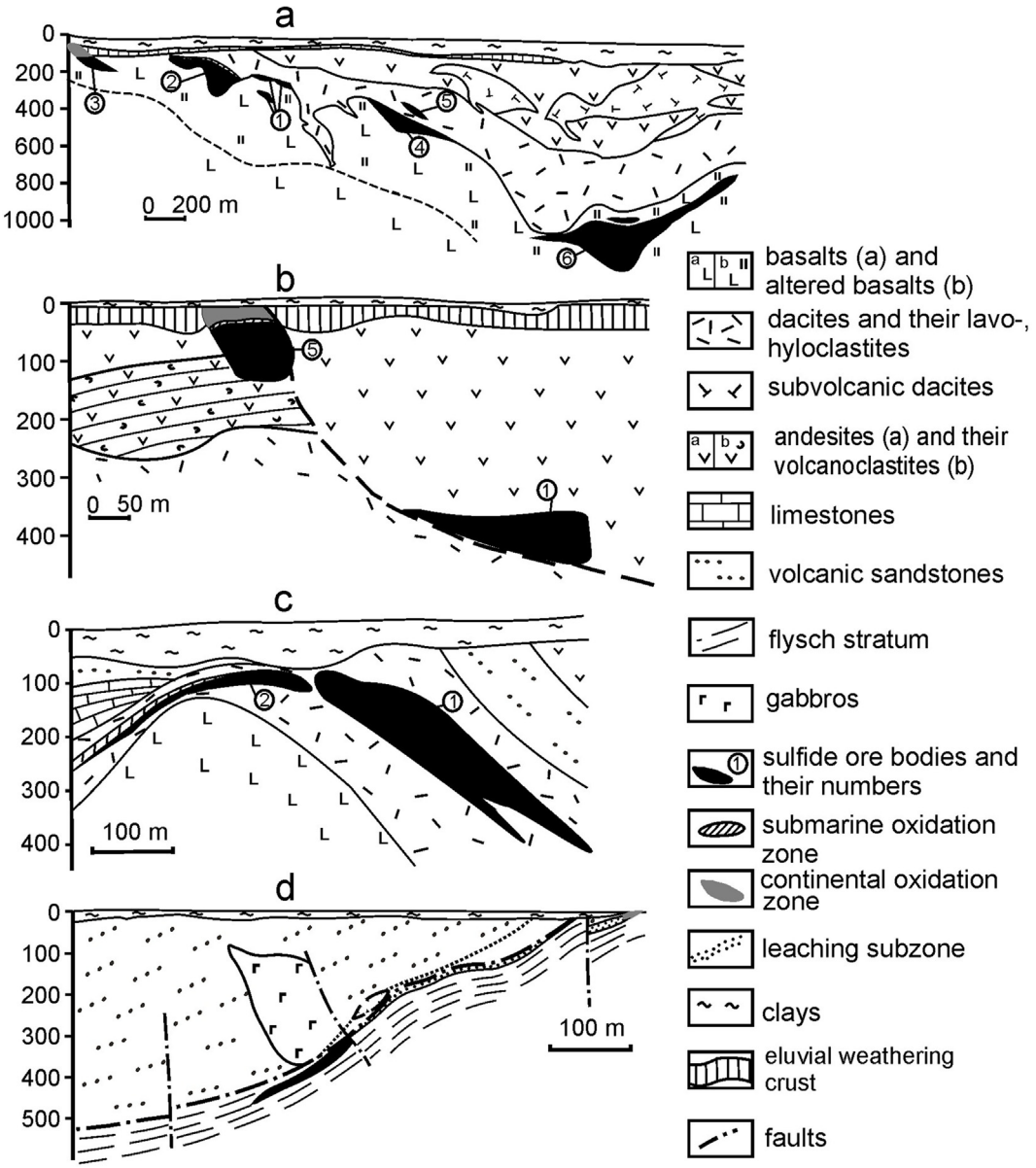

Fig. 2. Position of massive sulfide ore bodies of the Yubileynoe (a), Zapadno-Ozernoe (b), Molodezhnoe (c) and Amur (d) VHMS deposits of the Urals (modified after Prokin and Buslaev, 1999).

2.1. Light and electron microscopy

First, samples were studied by reflected light microscopy (Axiolab CZ, Axioscope A.1 and Olympus BX51 optical microscopes). The chemical composition of minerals was analyzed using scanning electron microscopes (SEM): a REMMA-202M SEM equipped with a Link ED-System operating at a 1 μm electron beam, a 15 nA beam current, a 20 kV accelerating voltage, a counting time of 120 s, and a Vega3 Tescan SEM equipped with an EDA X-Act Oxford instruments operating at a 3 μm electron beam, a 20 nA beam current, a 20 kV accelerating voltage and a counting time of 120 s. The standards are the MINM-25–53 from ASTIMEX Scientific Limited (mineral mount no. 01-044) and a registered standard no. 1362 (Microanalysis Consultants Ltd.).

2.2. Bulk analysis

The Se content in bulk samples was analyzed by atomic absorption on a Perkin-Elmer 3110 spectrometer (samples from continental oxidation zone) and inductively-coupled plasma mass spectrometry (ICP-MS) on an Agilent 7700× mass spectrometer calibrated against the USGS rock standard BCR-2 (samples from submarine oxidation zone).

The samples for ICP-MS analysis were digested in Teflon autoclaves using a mixture of HF, HCl and HNO_3 in a SpeedWave microwave digestion system (Berghof, Germany) during two-stage heating up to 180 °C for 40 min. After digestion, the fluorine complexes were decomposed by double evaporation of the dry residual with concentrated HNO3 at 110 °C in glassy carbon crucibles. The precipitates were further dissolved in hot 0.5 N HNO3 and reduced to a 100-ml aliquot. All the pure acids used for digestion were additionally purified in a BSB-939-IR apparatus (Berghof, Germany). The water for dilution was deionized in a Milli-Q® Integral Water Purification System (Millipore, US). The analytical uncertainties on individual trace elements are ≤5 rel.%.

2.3. Thermodynamic calculations

The Eh–pH diagrams we calculated using the Geochemist's Workbench (GMB 9.0) software package (Bethke and Yeakel, 2011) for

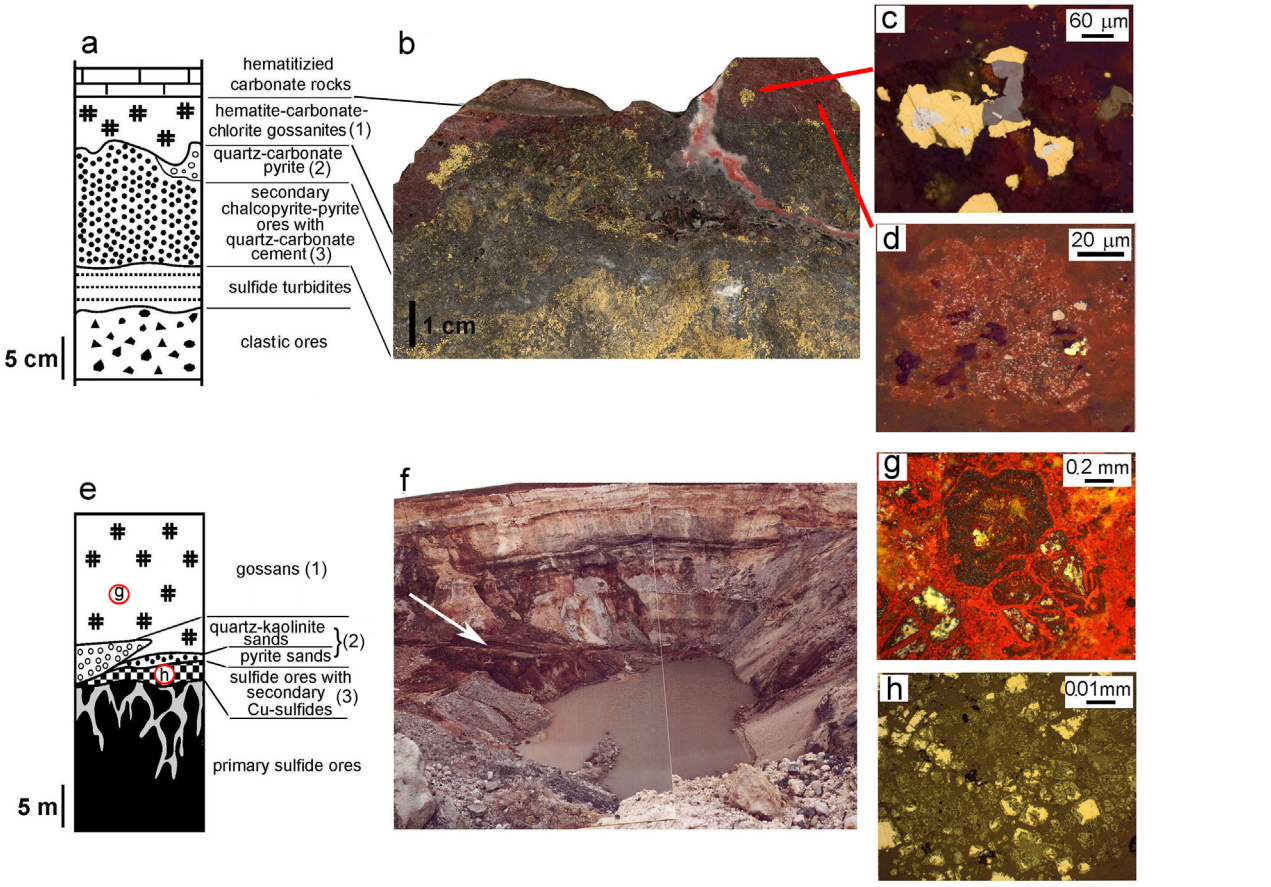

Fig. 3. Submarine and continental oxidation zones of Yubileynoe VHMS deposit. Submarine oxidation zone: a – lithological column, b – sample from oxidation zone, c – secondary chalcopyrite-sphalerite intergrowth with inclusions of Se-bearing galena, d – pseudomorphic hematite-quartz aggregate after sulfide clast. Continental oxidation zone: e – lithological column, f – open-pit with gossans (marked by arrow) and overlapping sedimentary thickness, g – microbreccia with goethite cement from iron hat, h – relic pyrite sand with secondary copper sulfides. Numbers of subzones correspond to the numbers of subzones in text. Position of the polished samples is shown by arrows (submarine oxidation zone) and by circles with corresponding characters (continental oxidation zone).

the average activities of components in waters formed in the oxidation zone:

$a_{\Sigma S} = 10^{-3}$, $a_{\Sigma Se} = 10^{-5}$, $a_{CO_2} = 10^{-2}$, $a_{\Sigma Fe} = 10^{-3}$, $a_{\Sigma Pb} = 10^{-7}$, $a_{\Sigma Hg} = 10^{-7}$, $a_{\Sigma Ag} = 10^{-7}$

(Krivovichev et al., 2011). The initial database contains the thermodynamic characteristics of 46 elements, 47 basis species, 48 redox couples, 551 aqueous species, 624 solid phases, and 10 gases recorded as equilibrium constants of dissociation reactions between particles in solutions and reactions of solid phase dissolution. The introduction of additional components into the database and the specification of some solubility products preceded the calculation of the diagrams. The activity coefficients we calculated from the Debye–Hückel equation. All diagrams we calculated for ambient conditions of 25 °C and 1 bar.

2.4. Geological outline of the deposits studied

The Urals fold belt is subdivided into several structural zones (Fig. 1), which reflect different geodynamic settings, including fragments of the former island arcs, inter-arc and back-arc basins and a possible marginal sea (Puchkov, 2017). The VHMS deposits formed in all these geodynamic settings since the Late Silurian to Middle Devonian (Prokin and Buslaev, 1999; Herrington et al., 2005; Puchkov, 2017). Most objects with Se minerals, including Yubileynoe, Zapadno-Ozernoe, Molodezhnoe, Kul-Yurt-Tau, Gai and Kaban-I deposits, are ascribed to the Uralian-type bimodal–mafic class of VHMS deposits (Prokin and Buslaev, 1999; Seravkin, 2010; Maslennikov et al., 2017). Because of host sedimentary complex, the Amur Zn deposit is referred to the SEDEX type of the deposits (Seravkin and Snachev, 2012), but semi-massive ore structures and negligible Pb content of ores bring it together with Besshi-type of the VHMS deposits (Puchkov, 2017). The Aleksandrinskoe and Dzhusa deposits are referred to the Kuroko-type (Puchkov, 2017).

2.5. Yubileynoe deposit

The Yubileynoe deposit occurs within the Lower Devonian Baymak–Buribay Formation in the West Magnitogorsk fore-arc region of an incipient oceanic paleoisland arc (Prokin and Buslaev, 1999; Zaykov et al., 2001; Herrington et al., 2005) (Fig. 1). The main ore bodies are underlain by altered basaltic pillow lavas and their breccias with disseminated chalcopyrite and pyrite and stockwork veins. In the hanging wall, the ore bodies are consequently covered by basaltic hyaloclastites, rhyolites, dacite lavas and andesitic basalts (Fig. 2a). The Mesozoic–Cenozoic sedimentary rocks overlap the Middle Devonian host volcanic rocks. The thickness of overlapping rocks reaches 130 m at the present-day erosion level (unpublished data of Tatarko, 1996).

Six lenticular massive sulfide ore bodies lie conformably within the wall rocks (Fig. 2a). Samples of submarine oxidation zone were collected from the top of Ore body no. 2 (Fig. 2a) and specimens of continental oxidation zone were collected above Ore bodies nos. 2 and 3, which were exploited by an open pit.

Ore body no. 2 was interpreted as a strongly eroded sulfide mound with massive pyrite and disseminated chalcopyrite in the mound core and sulfide breccias with fragments of smoker chimneys in the upper

part of the mound (Maslennikov et al., 2013). Sulfide turbidites are widespread at the flanks of the ore body (Maslennikov et al., 2014). Pyrite, chalcopyrite, and sphalerite are major minerals of massive sulfide ores. Rare minerals are marcasite, pyrrhotite, arsenopyrite, galena, tennantite, bornite, magnetite, hematite, electrum and native gold. Numerous tellurides associated with gold were found in relics of black and grey smoker chimneys, as well as in sulfide breccias and turbidites (Tseluyko et al., 2019).

The Se content of sulfide ores varies from 1 to 388 ppm (69 ppm, on average). According to LA-ICP-MS analysis, chalcopyrite, pyrite, and galena from chimneys of Ore body no. 2 have high average Se content (320, 353, and 1561 ppm, respectively). The Se content of late pyrite from pyrite-chalcopyrite aggregates in sulfide turbidites is 170–315 ppm (Maslennikov et al., 2014).

The submarine oxidation zone of the deposit consists of the following subzones (top to bottom): (1) an oxidation subzone with carbonate-bearing hematite–chlorite rocks (gossanites), occurring at the top and flanks of the ore body (Fig. 3a, b); (2) a leaching subzone with 4–5-cm thick quartz–carbonate layers and disseminated pyrite; and (3) a secondary copper enrichment subzone (similar to continental one) with chalcopyrite–bornite–sphalerite fragments and various tellurides (Fig. 3c). The replacement textures of hematite–chlorite aggregates after sulfide clasts and hyaloclasts indicates the clastic precursor of gossanites (Fig. 3d). Hematitized worm's microtubes (up to 200 μm in diameter) and bacteriomorphic textures are observed in submarine oxidation zone (Ayupova et al., 2018). Se-bearing galena, altaite, acanthite and uraninite have been found in authigenic chalcopyrite and hematite–chlorite–carbonate matrix of gossanites (Ayupova et al., 2018). The Se content of submarine oxidation zone varies from 40 to 220 ppm (Ayupova et al., 2017a).

The continental oxidation zone above Ore bodies nos. 2 and 3 began to form in the Triassic (unpublished data of Tatarko, 1996). The gossan paleosurface was eroded with subsequent formation of eluvial and talus sediments, which are locally characterized by economic Au content. Rare coral relics replaced by siderite were found in the upper part of the eroded gossans, indicating that continental supergene zone was covered by sea and benthos evolved on gossans. The Middle Jurassic lagoonal sedimentary rocks with lignite and coalified wood remnants overlap the Triassic supergene zone (Novoselov et al., 2019).

The structure of the oxidation zone of this deposit includes several subzones (top to bottom): (1) a 0–32 m thick iron cap subzone (gossans), (2) a 0–2 m thick leaching subzone with kaolinite-bearing barite–quartz–pyrite and quartz–pyrite sands, and (3) a 5–10 m thick secondary copper enrichment subzone, which ocassionally develops up to 30 m thick. Near-ore quartz–sericite alteration in the oxidation zone is transformed to quartz–kaolinite clay rocks (Fig. 3e and f).

The gossans are massive and ochrous; frequent clastic structures are inherited from sulfide ores. The average Se content of technological samples of oxidation products, including gossans, sands and secondary enriched ores, is 160 ppm (unpublished data of Tatarko, 1996). According to our data, the average content of Se in hand specimen of gossans is 120 ppm. Quartz, goethite, maghemite and siderite are major minerals of gossans (Fig. 3g). Native copper, gold and silver, secondary Au tellurides, pyrite, chalcopyrite (including Se-bearing variety), sphalerite, cuprite, malachite, azurite, and copper sulfates are minor and accessory.

The leaching subzone consists of sandy material with pyrite, quartz and barite relics (Fig. 3h). The average Se content is 8 ppm (unpublished data of Tatarko, 1996).

The secondary copper enrichment subzone is unevenly developed in the top of massive sulfide bodies. The minerals of the covellite and chalcocite groups often enriched in Se are major secondary minerals. Naumannite, tiemannite and clausthalite were found in assemblage with secondary copper sulfides.

2.6. Zapadno-Ozernoe deposit

The Zapadno-Ozernoe VHMS deposit is situated in the East Magnitogorsk paleoisland arc (Prokin and Buslaev, 1999). Massive sulfide ores are related to the Eifelian volcano-sedimentary sequences of the Karamalytash Formation and are overlapped by the Zhivetian volcanic rocks of the Ulutau Formation (Gavrilov et al., 1984) (Fig. 2b).

There are 15 massive sulfide bodies mostly composed of sulfide breccias and turbidites with minor amount (10%) of massive ores. The ores are characterized by Se high contents (up to 516 ppm) (Gavrilov et al., 1984). The oval-shaped Ore body no. 5, up to 12 m thick, is limited by faults. The porphyric andesites with minor quartz rhyolites, volcaniclastic rocks, and amygdaloidal basalts are main host rocks. The almost vertical main body of quartz rhyolites controls both massive sulfide ores and continental supergene zone of Ore body no. 5. Colloform pyrite and fine-grained chalcopyrite–sphalerite–pyrite aggregates with minor tennantite-tetrahedrite, galena and barite are dominant in Ore body no. 5 (Gavrilov et al., 1984; Belogub et al., 2003).

The submarine oxidation zone of the deposit consists of (top to bottom) (1) carbonate–magnetite and magnetite with pyrite-sphalerite (2) subzones (Ayupova and Tseluyko, 2013). The fine-grained pseudomorphic magnetite after tabular hematite crystals with chalcopyrite–sphalerite ore clasts forms a layer 0.5 m thick above the clastic sphalerite–pyrite ores (Fig. 4a–c). The thin carbonate–magnetite layers are sandwiched between sphalerite–pyrite and magnetite ores. Hematite and sphalerite in this layer are completely replaced by magnetite (Fig. 4d and e). Secondary (authigenic) chalcopyrite and pyrite in assemblage with native gold, hessite and Se-bearing galena were identified in carbonates. The Se content of magnetite ore reaches 184 ppm (Ayupova et al., 2017a).

The continental supergene profile of Ore body no. 5 consists of the following subzones (top to bottom): (1) an iron cap subzone (gossans); (2) a subzone of beudantite–barite–quartz ochres similar to a jarosite subzone; (3) a leaching subzone composed of quartz and quartz–barite sand; (4) a sooty subzone with newly formed chalcogenides, (5) a native sulfur subzone; (6) a subzone of pyrite sands; and (7) a cementation subzone with secondary copper sulfides unevenly developed on primary ores (Fig. 4f–h) (Belogub et al., 2003). A thin silica crust was established between relict pyrite and sooty sands or native sulfur lenses. The Se content reaches 77 and 577 ppm in native sulfur and secondary chalcogenide-bearing subzones, respectively, and decreases to < 10 ppm in gossans (Belogub et al., 2003). The newly formed pyrite, greigite, galena, sphalerite, metacinnabar, unidentified Se-bearing Cu- and Pb-Hg-Ag sulfosalts, native selenium, tiemannite, dzharkenite, clausthalite and naumannite were found in the oxidation zone of the deposit (Belogub et al., 2003, 2008).

2.7. Molodezhnoe deposit

The Molodezhnoe deposit is located in the East Magnitogorsk paleoisland arc (Prokin and Buslaev, 1999; Zaykov et al., 2001; Herrington et al., 2005). The lenticular ore body occurs among felsic volcanic rocks above the basaltic uplift of the lower part of the Givetian bimodal mafic sequence (Fig. 2c). The ore body has been interpreted as a strongly eroded sulfide mound (Maslennikov et al., 2012). Massive pyrite–chalcopyrite–sphalerite ores comprise the central part of the ore body, the top of which is crowned by ore breccias cemented by barite. The coarse-clastic sulfide breccias are abundant at the slopes of the ore body and the sulfide turbidites occur at the flanks. The sulfide breccias host fragments of colloform and granular pyrite, pyrite–-sphalerite–chalcopyrite black smoker chimneys, diffusers, and biomorphic ores. The sulfide breccias and turbidites are overlapped by thin layers of hematite–chlorite–quartz gossanites (Fig. 5a and b). No continental supergene zone was described at the deposit.

The variable Se content (30–252 ppm) of ores depends on the mineral ore types. In Cu-rich ores of the western flank of the ore body, the

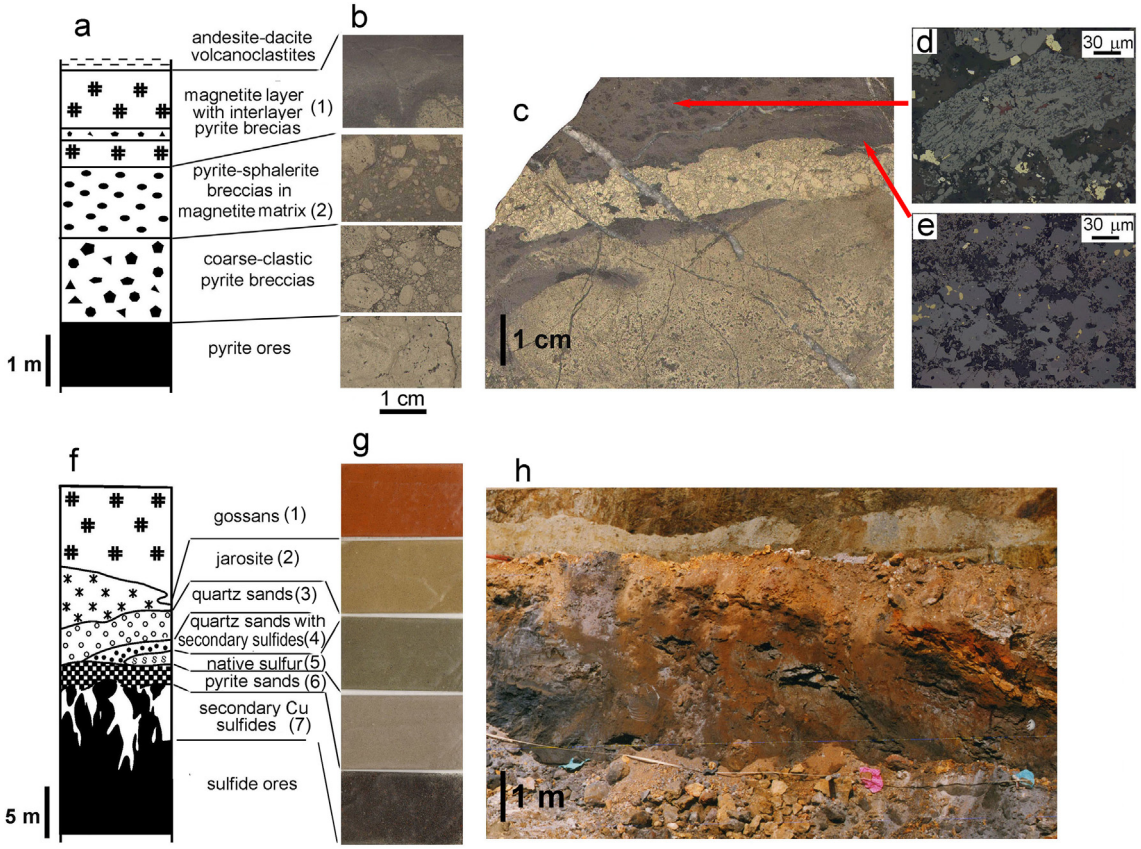

Fig. 4. Submarine and continental oxidation zones of Zapadno-Ozernoe VHMS deposit. Submarine zone: a – lithological column, b – samples of a, c – sample of magnetite ores, d – magnetite after hematite, e – magnetite after sphalerite. Continental oxidation zone: a – lithological column, g – probe of a, f – gossan outcrops in the open-pit. Numbers of subzones correspond to the numbers of subzones in text. Position of the polished samples is shown by arrows.

Se content is up to 252 ppm. The high Se contents are characteristic of hydrothermal minerals from smoker chimneys of the underlain fine-clastic pyrite–chalcopyrite–sphalerite ores: 106–1890 and 35–392 ppm Se in chalcopyrite and colloform pyrite, respectively (Ayupova et al., 2015).

The gossanites form dispersion halos around the eroded sulfide mound and cover an area several times larger than that of the ore bodies (Maslennikov et al., 2012; Ayupova et al., 2015). There are following subzones in the vertical section of the submarine oxidation profile (top to bottom): (1) an oxidation subzone with hematite and chlorite–hematite gossanites; (2) a leaching subzone with baritites and barite–hematite-quartz rocks; and (3) a secondary copper enrichment subzone with bornite or chalcopyrite (Fig. 5a). Numerous pseudomorphoses of hematite after sulfide clasts are described in gossanites (Fig. 5c). Strongly altered thin sulfide turbidite layers are locally enriched in secondary (authigenic) chalcopyrite, tennantite, barite, and bornite (Fig. 5d).

The Se content of gossanites varies from 30 to 334 ppm and reaches

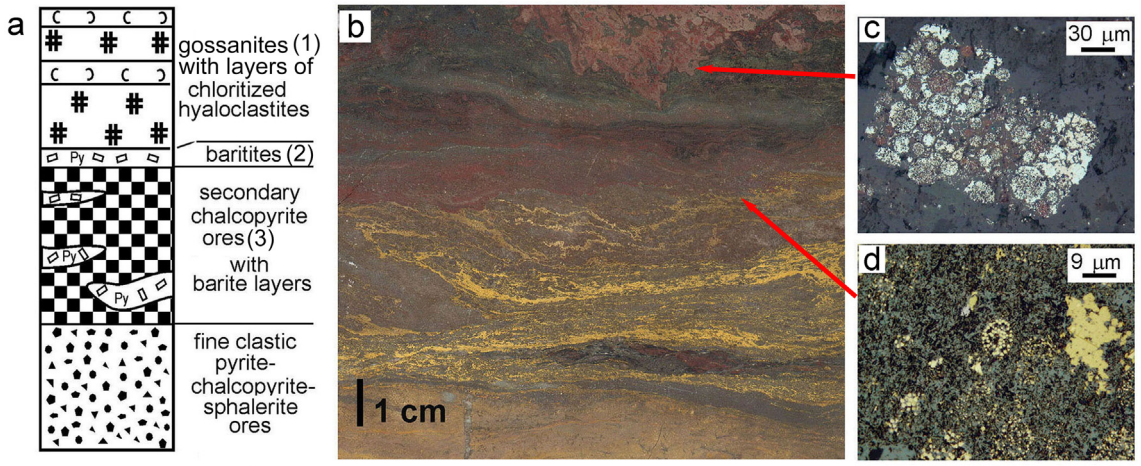

Fig. 5. Submarine oxidation zone of Molodezhnoe VHMS deposits. a – lithological column, b – sample from submarine zone, c – hematite after framboidal pyrite clast, d – hematite–secondary chalcopyrite–framboidal pyrite assemblages in gossanite. Numbers of subzones correspond to the numbers of subzones in text. Position of the polished samples is shown by arrows.

its maximum in the secondary copper enrichment subzone (up to 1352 ppm). The Se content of gossanites correlates with high contents of Ag), Pb, and Au (up to 987, 762, and 25 ppm, respactively) (Ayupova et al., 2017a). The Se minerals (clausthalite, naumannite (including its Te-bearing variety), bohdanowiczite, Se-bearing galena, roquesite) were found in chalcopyrite–pyrite–(bornite)–tennantite layers, where pyrite is intensely replaced by chalcopyrite, and in authigenic chalcopyrite, which is replaced by tennantite, bornite and barite (Ayupova et al., 2015). The Se minerals rarely occur in assemblage with chalcopyrite and galena in matrix of hematite–chlorite–quartz gossanites.

2.8. Amur deposit

The Amur Zn deposit is located at the junction of the East Magnitogorsk and East Uralian paleovolcanic zones (Herrington et al., 2005; Puchkov, 2017). The underlying sedimentary units and host rocks are metasiltstones and metapelites with the carbon-rich shales and limestones (Fig. 2d). The overlapping volcaniclastic mafic rocks with gabbro intrusions are thrust on the host rocks. The primary sulfide ores form lenticular bodies. According to our data, the maximum Se content of ores is 24 ppm (5.5 ppm, on average).

The ores exhibit banded structures with relict vertical grading of clasts and local stringer-disseminated structures. Sphalerite, pyrite and pyrrhotite are major ore minerals. Galena, chalcopyrite, arsenopyrite, ulmannite, jordanite, tennantite, boulangerite, unidentified Ag–Pb sulfosalts, and Hg-bearing electrum are minor. No submarine oxidation zone was identified at the deposit.

The continental oxidation zone is developed along a thrust fault and reaches more than 300 m deep (Fig. 6). The oxidation zone contains (top to bottom): (1) an iron cap subzone with cavernous (1a) and ocher (1b) gossans; (2) a leaching subzone with quartz and quartz–dolomite sands in the upper part and quartz–pyrite sand in the lower part; and (3) clayey rocks after volcaniclastic rocks along the thrust zone (Fig. 6a and b). The Se content of gossans varies from 0.2 to 17 ppm (our data). Tiemannite and clausthalite were found in the lower part of the ocher gossans at the boundary with the leaching subzone (Fig. 6c).

2.9. Other deposits mentioned in the text

The Kaban-I deposit, located in the Central Urals, belongs to the Kaban group of the VHMS deposits and is confined to the Tagil paleoisland arc. The deposit is associated with the rhyolite–basalt complex (Vikentyev et al., 2017). Pyrite and chalcopyrite are main ore minerals; sphalerite, arsenopyrite, tennantite and galena are secondary in abundance. Rare minerals are bornite, enargite and “orange bornite”. The continental oxidation zone of the deposit with (top to bottom) iron cap, leaching (quartz and pyrite sands) and secondary copper enrichment subzones was exploited in 2013 for gold recovery. Native selenium was found in pyrite and quartz sands (Blinov and Butnyakov, 2016). No submarine oxidation zone has been described at the deposit.

Detailed geological description of the Aleksandrinskoe deposit is given in (Vikentyev et al., 2017; Maslennikov et al., 2017). The deposit located in East-Magnitigorsk paleoisland arc and associated with the bimodal rhyolite-basalt complex. Typically, the Kuroko-type deposits in the Urals lack Fe-rich gossanites except for the Aleksandrinskoe deposit, where Fe-rich hematite–chlorite–carbonate gossanites (oxidation subzone) are intercalated with barite, sulfides and calcareous hyaloclastic lenses. The gossanites contain native gold, tetradymite (0.53–0.66 wt% Se), tsumoite (up to 0.53 wt% Se), rucklidgeite (up to 1.1 wt% Se), hessite and altaite included in pseudomorphic hematite after pyrite, chalcopyrite and sphalerite clasts (Ayupova, 2016; Maslennikov et al., 2019). Continental oxidation zone of the deposit includes (top to bottom) iron cap, jarosite, leaching (quartz, quartz-barite and pyrite sands) and secondary Cu-enrichment subzones. No Se minerals have been found in continental oxidation zone of the deposit (Belogub, 2009).

Guy and Kul-Yurt-Tau deposits are confined to West-Magnitogorsk paleoisland arc (Prokin and Buslaev, 1999; Puchkov, 2017). Giant Guy deposit locates in rhyolite-basalt volcanic complex. Structure, geochemistry and mineralogy of the continental oxidation zone of the deposit is given in (Zaykov and Sergeev, 1993). Pyrite bodies of small Kul-Yurt-Tau deposit locate between basalt-andesibasalt and rhyodacite (Zaykov et al., 1987) The continental oxidation zone of the deposit was completely developed in the 50 s and described in (Paley, 1957).

2.10. Se minerals in the oxidation zones of the Urals VHMS deposits: new data

The morphology of secondary chalcogenides, such as skeletal crystals, druses on cavity walls or corroded primary sulfides, and veinlets in goethite or hematite and magnetite, is a key criterion for the identification of secondary origin of minerals.

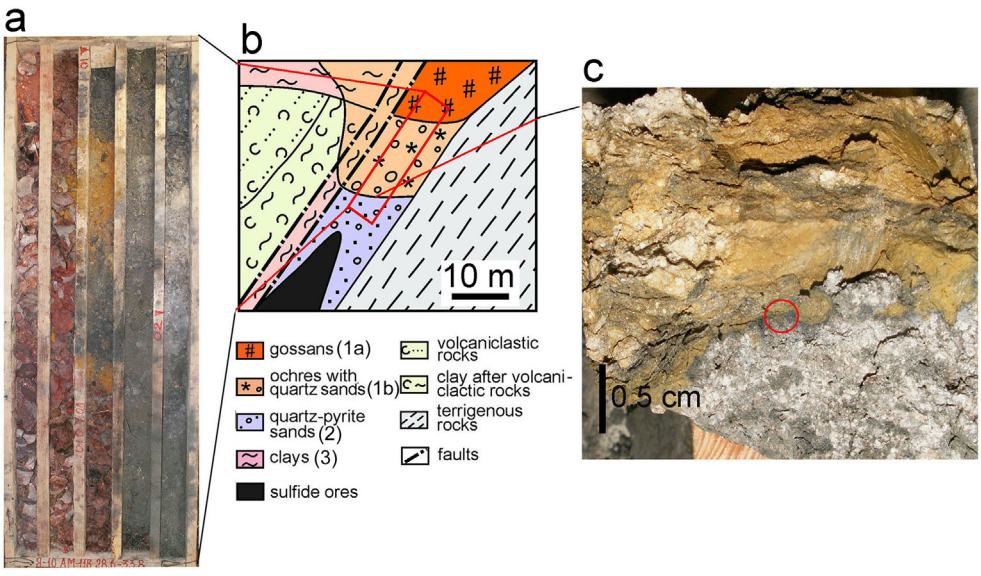

Fig. 6. Continental oxidation zone of Amur deposit: a – core samples, b – schematic cross-section, c – sample from the boundary between leached zone of relic quartz, barite and rare pyrite and sooty limonite ochre. The circle marks the position of the selenides find. Numbers of subzones correspond to the numbers of subzones in text.

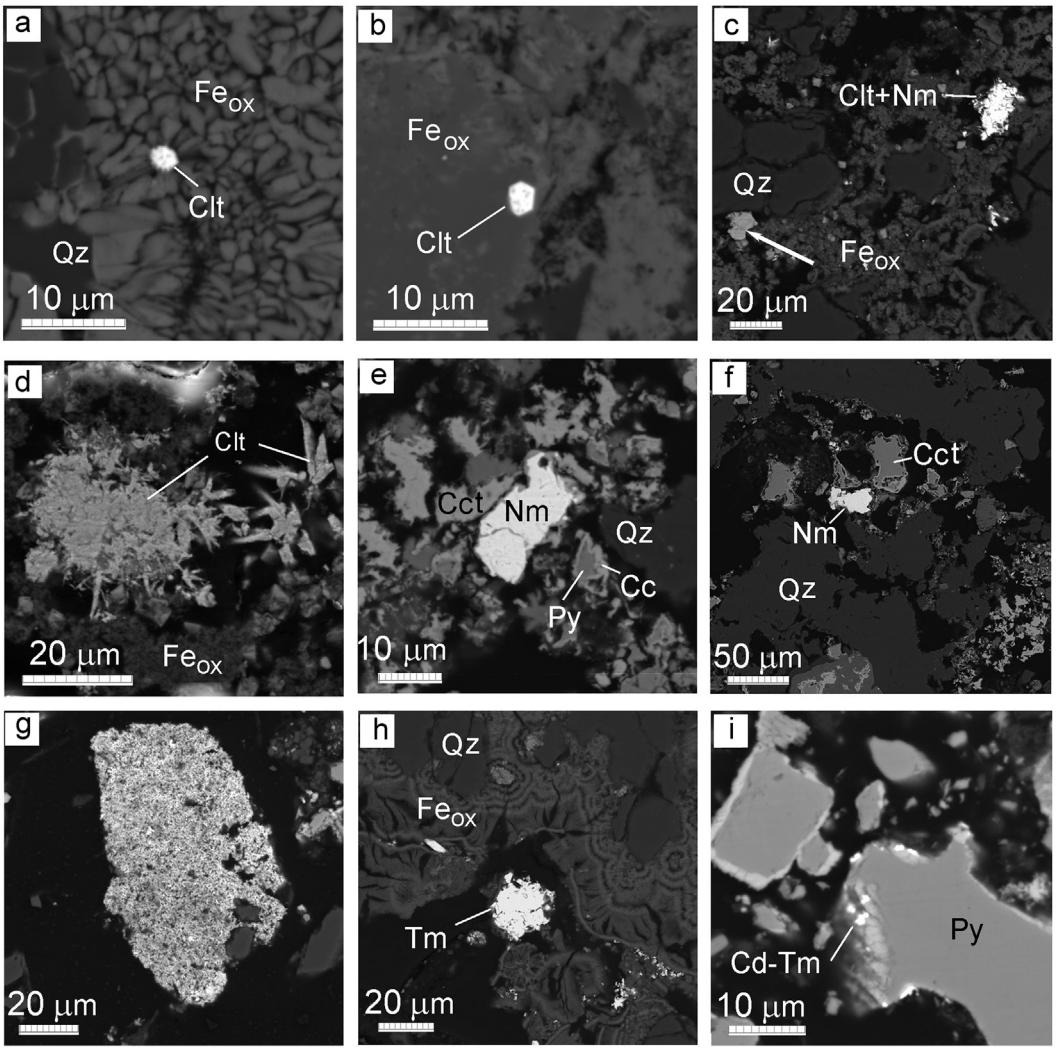

Fig. 7. Selenides in the continental oxidation zone of Yubileynoe (a, b, c, e, f, i) and Amur (d, g, h) deposits: a–b – clausthalite crystals within limonite, c – clausthalite-naumannite fine aggregate in limonite with quartz relics, arrow – native brass, d – radial aggregate of clausthalite crystals from the cave of ironstone, e – naumannite and secondary copper sulfides with pyrite relics, f – naumannite with Se-enriched secondary copper sulfides in sooty sand, g – fine intergrowth of naumannite and tiemannite in sooty sand, h – tiemannite in the cave in colloform limonite; i – Cd-bearing tiemannite, associated with secondary copper sulfides at the relic pyrite surface. BSE-photo. Chp – chalcopyrite, Py – pyrite, Clt – clausthalite, Nm – naumannite, Tm – tiemannite, Cc – chalcocite, Fe_{ox} – limonite and goethite, Q – quartz.

2.11. Clausthalite (PbSe) and Se-bearing galena (Pb(S,Se))

2.11.1. Continental oxidation zone

At the Yubileynoe deposit, fine clausthalite crystals 1–2 μm in size are found in continental gossans (Fig. 7a and b). The intimate intergrowths of clausthalite and naumannite in assemblage with native brass were also found in pyrite sand, which hosts secondary copper sulfides (Fig. 7c). Clausthalite from this deposit occasionally contains Fe (Table 1).

At the Amur deposit, the radial intergrowths of hastate clausthalite crystals occur in limonite cavities at the boundary with relic quartz–-sulfide sand (Fig. 7d). Clausthalite locally contains Fe (Table 1). Similar hastate aggregates are also made up of secondary galena in the sooty subzone of the Zapadno-Ozernoe deposit (Belogub et al., 2003).

2.11.2. Submarine oxidation zone

At the Zapadno-Ozernoe deposit, numerous grains of Se-bearing galena (4.00–5.53 wt% Se, Table 1) and extremely rare anhedral clausthalite grains are associated with authigenic chalcopyrite and pyrite in quartz–carbonate matrix of the magnetite layers (Fig. 8a–c). One analysis of galena exhibits 15.18 wt% Se and corresponds to an intermediate member of the galena–clausthalite isomorphic series (Table 1).

At the Molodezhnoe deposit, clausthalite forms anhedral inclusions 3–4 μm in size in authigenic chalcopyrite–tennantite–pyrite aggregates and at contacts with barite, where the size of clausthalite grains reaches 40 μm. Typically, clausthalite is associated with shtromeyerite and Se-bearing minerals: naumannite (including Te-bearing variety), Se-bearing galena (up to 4–8 wt% Se), roquesite, and bohdanowiczite (Fig. 8d–g). Locally, clausthalite replaces naumannite (Fig. 8f). The presence of Ag (up to 6.73 wt%) is a specific feature of chemical composition of clausthalite from this deposit (Table 1).

At the Yubileynoe deposit, relatively large (~50 μm) clausthalite aggregates in assemblage with cervelleite were found in authigenic chalcopyrite of secondary enrichment subzone (Fig. 8h). Small inclusions of Se-bearing galena (up to 2.52 wt% Se, Table 1) associated with electrum are observed in chalcopyrite of hematite–carbonate–chlorite gossanites.

Table 1
Chemical composition (wt.%) of secondary Se-bearing galena and clausthalite (wt.%).

Pb	S	Se	As	Sb	Hg	Fe	Cu	Ag	Σ	Formula (S + Se = 1.00)
Continental oxidation zone										
Yubileynoe deposit										
Claysthalite inclusion within limonite aggregates										
69.47	–	27.10	–	–	–	3.42	–	–	100.00	
Amur deposit (Blinov, 2015)										
Aggregates of clausthalite crystals in limonite cavities										
71.82	–	28.18	–	–	–	–	–	–	100.00	$Pb_{0.97}Se_{1.00}$
70.79	–	28.17	–	–	–	1.05	–	–	100.01	$Pb_{0.96}Se_{1.00}$
72.22	–	27.48	–	–	–	–	–	–	99.70	$Pb_{1.00}Se_{1.00}$
Submarine oxidation zone										
Yubileynoe deposit										
Se-bearing galena in carbonate–hematite matrix										
85.22	12.79	1.99	–	–	–	–	–		100.00	$Pb_{0.97}(S_{0.94}Se_{0.06})_{1.00}$
85.24	12.25	2.52	–	–	–	–	–		100.01	$Pb_{0.99}(S_{0.92}Se_{0.08})_{1.00}$
Zapadno-Ozernoe deposit										
78.42	6.39	15.18	–	–	–	–	–	–	99.99	$Pb_{0.97}(S_{0.51}Se_{0.49})_{1.00}$
Se-bearing galena associated with magnetite										
84.10	11.31	4.58	–	–	–	–	–	–	99.99	$Pb_{0.99}(S_{0.86}Se_{0.14})_{1.00}$
83.87	11.07	5.07	–	–	–	–	–	–	100.01	$Pb_{0.99}(S_{0.84}Se_{0.16})_{1.00}$
83.51	10.96	5.53	–	–	–	–	–	–	100.00	$Pb_{0.98}(S_{0.83}Se_{0.17})_{1.00}$
83.51	11.59	4.90	–	–	–	–	–	–	100.00	$Pb_{0.95}(S_{0.85}Se_{0.15})_{1.00}$
84.24	11.76	4.00	–	–	–	–	–	–	100.00	$Pb_{0.97}(S_{0.88}Se_{0.12})_{1.00}$
84.49	11.31	4.20	–	–	–	–	–	–	100.00	$Pb_{1.00}(S_{0.87}Se_{0.13})_{1.00}$
Molodezhnoe deposit										
Clausthalite at the contact of sulfides and barite										
72.57	1.49	25.23	–	–	–	–	–	0.71	100.00	$(Pb_{0.96}Ag_{0.02})_{0.98}(Se_{0.13}S_{0.87})_{1.00}$
69.83	–	27.96	–	–	–	–	–	1.93	99.72	$(Pb_{0.95}Ag_{0.05})_{1.00}Se_{1.00}$
70.57	–	27.96	–	–	–	–	–	1.47	100.00	$(Pb_{0.96}Ag_{0.04})_{1.00}Se_{1.00}$
69.84	–	28.76	–	–	–	–	–	1.40	100.00	$(Pb_{0.93}Ag_{0.04})_{0.97}Se_{1.00}$
67.94	–	29.14	–	–	–	–	–	3.54	100.62	$(Pb_{0.89}Ag_{0.09})_{0.98}Se_{1.00}$
69.86	–	27.14	–	–	–	–	–	2.04	99.04	$(Pb_{0.98}Ag_{0.06})_{0.94}Se_{1.00}$

Note. Dash, not detected.

3. Naumannite (Ag_2Se)

3.1. Continental oxidation zone

At the Yubileynoe deposit, naumannite forms anhedral grains up to 5 μm in size in sooty sands, which consist of corroded pyrite and secondary copper sulfides. Most naumannite grains were found in a thin layer of the fine-grained bluish sooty sand clamped between gossan and relic pyrite sand. Naumannite grains are often associated with chalcocite (Fig. 7e and f) and locally occurs as relics in secondary copper sulfides. Naumannite exhibits a small excess of Ag in chemical composition (Table 2).

At the Amur deposit, the intimate intergrowth of naumannite and tiemannite up to 60 μm in size are identified in relic quartz–pyrite sands and in the cavities of gossans (Fig. 7g, Table 2).

3.1.1. Submarine oxidation zone

Naumannite was established in gossanites of the Molodezhnoe deposit. It forms rare anhedral inclusions up to 10 μm in size in authigenic chalcopyrite and tennantite and typically replaces clausthalite (Fig. 8f). The composition of naumannite is close to theoretical (Table 2). The submarine oxidation zone only of this deposit contains a Te-rich variety of naumannite (2.23–23.15 wt% Te, Table 2). It forms anhedral inclusions up to 10–15 μm in size in authigenic chalcopyrite and tennantite and, along with clausthalite and bohdanowiczite, occurs at the contact between sulfides and barite or hematite. One analysis of the mineral with Ag/(Se + Te) ratio of 1.74 (Table 2) exhibits deficit of Ag and is similar to a possible Se analogue of stützite rather than of naumannite.

3.1.2. Tiemannite (HgSe)

At the Amur deposit, anhedral tiemannite grains up to 3 μm in size intergrown with naumannite (Fig. 7h) were found in relic quartz–pyrite sand with clay minerals and limonite. Mineral contains Se 28.23 wt%, Hg 71.77 wt%. At the Yubileynoe deposit, tiemannite is closely associated with secondary copper sulfides and naumannite in sooty sand. The Cd-rich tiemannite grains few micrometers in size were found on the surface of corroded pyrite in relic pyrite sands (Fig. 7i). The mineral was identified using ED spectrum.

3.1.3. Bohdanowiczite ($AgBiSe_2$)

Bohdanowiczite is a very rare mineral found only in the submarine oxidation zone of the Molodezhnoe deposit in assemblage with clausthalite (Fig. 8g). Its chemical composition is close to theoretical (Table 3).

4. Se-bearing sulfides and sulfosalts

4.1. Continental oxidation zone

Copper sulfides (covellite and chalcocite) are most abundant secondary minerals of the cementation subzone of continental oxidation zone. At the Yubileynoe deposit, these minerals contain up to 8 wt% Se (Table 4) and are characterized by uneven Se distribution. The Se-free chalcocite and covellite are associated with naumannite and clausthalite, whereas Se-bearing copper sulfides occur in assemblage with tiemannite. The Se-bearing copper sulfides grow on oxidized pyrite and form interstitial aggregates between relic minerals. Both types of supergene copper sulfides also form euhedral or anhedral inclusions in siderite and goethite and are characterized by variable Fe content (from nill to 8.08 wt%). The (Cu + Fe)/(S + Se) ratio of secondary copper sulfides varies from 1.16:1 to 1.82:1.

The Se-bearing chalcopyrite (a member of the chalcopyrite $CuFeS_2$–eskebornite $CuFeSe_2$ series) is abundant in gossans of the Yubileynoe deposit. Secondary chalcopyrite forms small (max 10 μm in size) druses in cavities of goethite and siderite (Fig. 9a–d) and at the contacts between these minerals (Fig. 9e and f). Some chalcopyrite

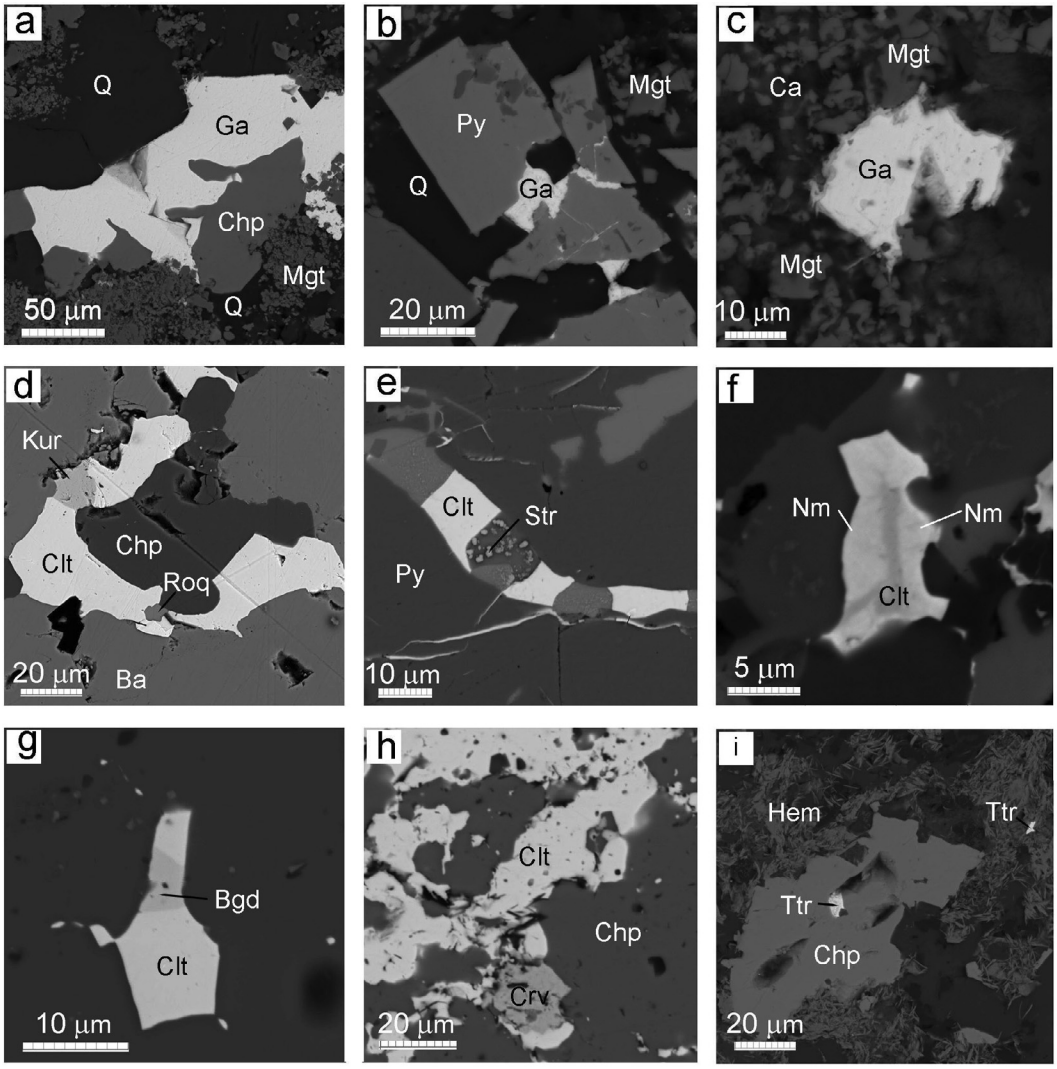

Fig. 8. Selenides and Se-bearing sulfides in the submarine oxidation zones of Zapadno-Ozernoe (a–c), Molodezhnoe (d–g), Yubileynoe (h) and Alexandrinskoe (i) deposits: a–c: Se-bearing galena associated with secondary chalcopyrite within magnetite ores; d – clausthalite, kurilite and roquesite assemblages at the contact of chalcopyrite and barite; e – diagenetic vein with clausthalite, tennantite and shtromeyerite within pyrite, f – naumannite-clausthalite assemblages at the contact of barite and pyrite; g – intergrowth of clausthalite and bohdanowiczite within chalcopyrite; h – clausthalite and cervelleite within secondary chalcopyrite; i – selenium tetradymite within secondary chalcopyrite. BSE-photo. Ba – barite, Tn – tennantite, Mgt – magnetite, Hem – hematite, Ga – selenium bearing galena, Kur – kurilite, Roq – roquesite, Bgd – bohdanowiczite, Ttr – tetradymite, Crv – cervelleite. Other abbreviation see Fig. 7.

grains are host to Cu-bearing gold (Fig. 10a), Se-bearing sphalerite and bornite. Locally, chalcopyrite occurs along the growth zones of goethite nodules (Fig. 10b) or forms aggregates in Fe chlorite (Fig. 10c). The Se content of chalcopyrite varies even within one grain from nil to 11.02 wt% (Table 4).

The Se- and Fe-bearing sphalerite (2.35 wt% Se, 5.56 wt% Fe) was found as inclusions of 10–15 μm in size in secondary chalcopyrite at the Yubileynoe deposit.

4.1.1. Submarine oxidation zone

The Se-bearing roquesite $CuInS_2$ was found in the submarine oxidation zone of the Molodezhnoe deposit for the first time in the Urals VHMS deposits (Ayupova et al., 2017a). It forms isometric aggregates up to 12 μm in size in assemblage with clausthalite and tiny platy inclusions in clausthalite of the secondary copper enrichment subzone (Fig. 8d). Rare roquesite grains are associated with chalcopyrite in the hematite subzone. Roquesite contains up to 4.47 wt% Se (see Table 3) and up to 10.02 wt% Pb.

5. Discussion

5.1. Diversity of Se minerals in continental and submarine oxidation zones

The data on supergene selenides and Se-bearing chalcogenides from the Urals VHMS deposits are summarized in Table 5.

Native selenium was described first amid Se minerals of the South Urals VHMS deposit. It was found as centimeter-in-size fine-grained lenses in the native sulfur subzone of the continental oxidation zone of the Kul-Yurt-Tau deposit (Paley, 1957). Later, similar occurrence of native selenium was reported for the Gai (Zaykov and Sergeev, 1993), Zapadno-Ozernoe (Belogub et al., 2003), and Kaban-I (Blinov and Butnyakov, 2016) deposits, where it was found as minute-size grains in sulfur sand (Gai) or pyrite and quartz sands (Kaban-I) and within Se-bearing pyrite–dzharkenite zonal aggregates (Zapadno-Ozernoe). No native selenium was found in submarine oxidation zones of the deposits studied.

Clausthalite and Se-bearing galena are most abundant Se minerals both in the continental and submarine oxidation zones (Table 5). In the continental oxidation zone, it typically forms small grains associated

Table 2
Chemical composition of naumannite (wt %) from continental and submarine oxidation zones.

Se	Te	Fe	Ag	Formula (Se + Te = 1.00)
Yubileynoe deposit, continental oxidation zone				
26.27	–	–	73.73	$Ag_{2.05}Se_{1.00}$
26.74	–	–	73.26	$Ag_{2.01}Se_{1.00}$
26.07	–	–	73.93	$Ag_{2.08}Se_{1.00}$
Amur deposit, continental oxidation zone				
28.26	–	0.72	70.99	$Ag_{2.05}Se_{1.00}$
Molodezhnoe deposit, submarine oxidation zone				
27.01	–	–	72.85	Ag1.97Se1.00
26.67	–	–	72.33	Ag1.99Se1.00
26.85	–	–	73.15	Ag1.99Se1.00
26.39	2.23	–	71.02	Ag1.87(Se0.95Te0.05)
16.73	14.65	–	68.61	Ag1.95(Se0.65Te0.35)2.00
14.53	17.96	–	68.17	Ag1.95(Se0.57Te0.43)2.00
16.87	14.32	–	68.82	Ag1.82(Se0.66Te0.34)2.00
10.58	23.15	–	66.27	Ag1.95(Se0.58Te0.42)2.00
17.17	14.59	–	68.24	Ag1.91(Se0.66Te0.34)2.00
15.45	15.59	–	69.79	Ag2.04(Se0.62Te0.38)2.00
23.27	6.61	–	69.78	Ag1.87(Se0.85Te0.15)2.00
15.69	18.90	–	65.10	$Ag_{1.74}(Se_{0.57}Te_{0.43})_{2.00}$

Note. Dash, not detected.

with other selenides in the lower horizons or euhedral (including skeletal) crystals in gossans or at the boundary between leaching subzone and gossan. At the Kaban-I deposit, clausthalite is associated with native selenium (Blinov and Butnyakov, 2016). At the Zapadno-Ozernoe deposit, it occurs in the siliceous crust between relic pyrite sand and sooty sand with secondary sulfides, native selenium, dzharkenite and rare tiemannite (Belogub et al., 2003). Skeletal clausthalite crystals were found at the Dzhusa deposit in association with secondary Se-bearing galena (Belogub et al., 2008), and Amur deposit, where it forms aggregates at the cavities wall of goethite. In submarine oxidation zones of Zapadno-Ozernoe, Molodezhnoe and Yubileynoe deposits, clausthalite and/or Se-bearing galena are always associated with secondary chalcopyrite, and, rarely, Se-bearing sulfides.

Naumannite also is a common secondary selenide of the oxidation zones of the South Urals VHMS deposits. In continental oxidation zone, it typically occurs in relic pyrite sands of the leaching subzone and secondary copper enrichment subzone. It was first found at the Yubileynoe deposit (unpublished data of Tatarko, 1996). According to our data, naumannite of this deposit is associated with tiemannite and Se-bearing secondary Cu sulfides. Naumannite associated with dzharkenite and native selenium was identified in pyrite sands of the Zapadno-Ozernoe deposit (Belogub et al., 2003). At the Kaban-I deposit, naumannite in assemblage with native selenium and cassiterite was recognized only in pyrite sand (Blinov and Butnyakov, 2016). In submarine gossanites, naumannite was found only at the Molodezhnoe deposit.

Table 4
Chemical composition (wt%) of secondary copper sulfides and chalcopyrite from continental oxidation zone of the Yubileynoe deposit.

Cu	Fe	S	Se	Crystal formula
Secondary copper sulfides				
70.78	–	19.36	3.87	$Cu_{1.70}(S_{0.93}Se_{0.07})_{1.00}$
61.90	8.08	28.88	1.14	$(Cu_{1.06}Fe_{0.16})_{1.22}(S_{0.98}Se_{0.02})_{1.00}$
73.50	1.92	22.67	1.66	$(Cu_{1.06}Fe_{0.16})_{1.22}(S_{0.97}Se_{0.03})_{1.00}$
75.23	2.69	22.08	–	$(Cu_{1.72}Fe_{0.07})_{1.79}S_{1.00}$
70.53	4.94	23.94	0.6	$(Cu_{1.47}Fe_{0.12})_{1.59}(S_{0.99}Se_{0.01})_{1.00}$
76.36	1.75	21.57	0.32	$(Cu_{1.77}Fe_{0.05})_{1.82}(S_{0.99}Se_{0.01})_{1.00}$
57.95	7.75	25.42	8.88	$(Cu_{1.01}Fe_{0.15})_{1.16}(S_{0.88}Se_{0.12})_{1.00}$
Chalcopyrite				
34.83	29.96	32.41	1.93	$Cu_{1.06}Fe_{1.03}(S_{1.95}Se_{0.05})_{2.00}$
36.13	28.00	31.42	4.55	$Cu_{1.09}Fe_{0.96}(S_{1.89}Se_{0.11})_{2.00}$
27.11	31.01	27.11	11.02	$Cu_{0.86}Fe_{1.13}(S_{1.72}Se_{0.28})_{2.00}$
31.31	28.64	27.98	5.21	$Cu_{1.05}Fe_{1.09}(S_{1.86}Se_{0.14})_{2.00}$

Note. Dash, not detected.

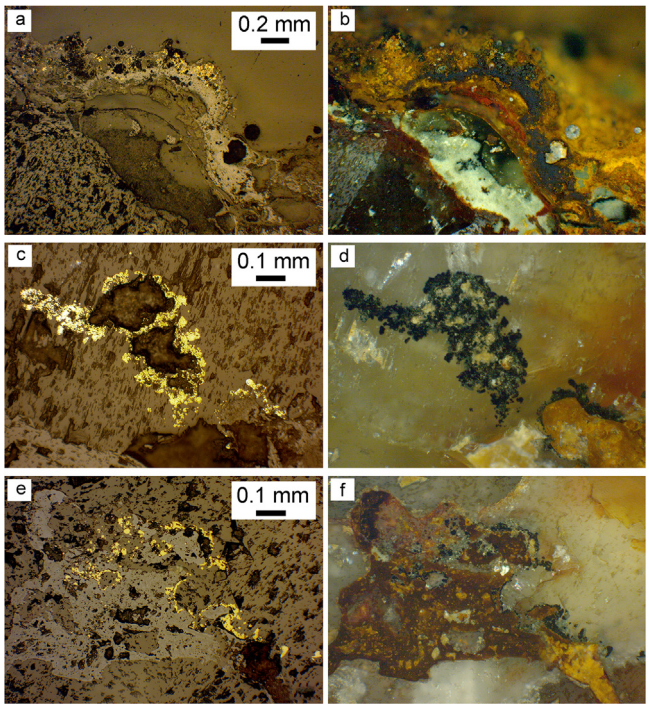

Fig. 9. Se-bearing chalcopyrite (yellow) in goethite of the Yubileynoe deposit: a–c – microdruse on the goethite surface (a-b) and cavity in siderite (c-d), e, f – at the contact between goethite and siderite. Left – reflected light, right – oblique light. (For interpretation of the references to colour in this figure legend, the reader is referred to the web version of this article.)

Tiemannite is relatively rare selenide and was found in continental oxidation zone only. First, tiemannite and "onofrite" (Hg sulfoselenide) were described by Zaykov and Sergeev (1993) in native sulfur sand

Table 3
Chemical composition (wt%) of bohdanowitzite (1, 2, Aleksandrinskoe deposit) and roquesite (3–7, Molodezhnoe deposit) from submarine oxidation zone.

No	Cu	In	Pb	Ag	Bi	Fe	Se	S	Σ	Crystal formula
1	–	–	–	22.32	46.09	–	31.58	–	99.99	$Ag_{1.03}Bi_{1.10}Se_{2.00}$
2	–	–	–	23.69	44.23	–	32.09	–	100.01	$Ag_{1.08}Bi_{1.04}Se_{2.00}$
3	25.76	44.60	–	–	–	1.53	4.47	23.64	100.00	$(Cu_{1.02}In_{0.98}Fe_{0.07})_{2.07}(S_{1.86}Se_{0.14})_{2.00}$
4	26.60	41.88	–	–	–	3.54	2.91	25.07	100.00	$(Cu_{1.02}In_{0.90}Fe_{0.15})_{2.05}(S_{1.91}Se_{0.09})_{2.00}$
5	25.67	44.91	–	–	–	0.98	4.42	24.01	99.99	$(Cu_{1.00}In_{0.98}Fe_{0.04})_{2.02}(S_{1.86}Se_{0.14})_{2.00}$
6	22.00	46.41	2.28	–	–	1.42	1.45	26.27	99.83	$(Cu_{0.83}In_{0.97}Fe_{0.06}Pb_{0.03})_{1.88}(S_{1.96}Se_{0.04})_{2.00}$
7	17.12	42.37	10.02	–	–	2.82	3.30	23.96	99.59	$(Cu_{0.68}In_{0.94}Fe_{0.13}Pb_{0.12})_{1.87}(S_{1.96}Se_{0.04})_{2.00}$

Note. Dash, not detected.

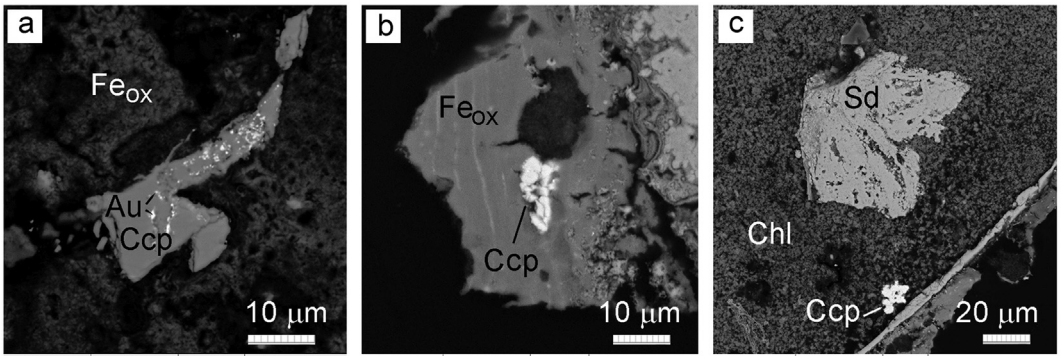

Fig. 10. Se-bearing chalcopyrite from the ironstone of Yubileynoe deposit: a – with inclusion of cuprian gold, b - within zonal nodule of goethite, c – crystal aggregate in chlorite mass with siderite. BSE-photo. Au – cuprian gold, Chl – chlorite, Sid - siderite. Other abbreviation see Fig. 7.

Table 5
Se minerals in continental and submarine oxidation zones of the Urals VMS deposits.

VHMS deposits	Continental oxidation zone	Submarine oxidation zone
Kul-Yurt-Tau (Paley, 1957)	Native selenium	
Gai (Zaykov and Sergeev, 1993; Sergeev et al., 1994)	Native selenium, tiemannite, yutenbogaardite, Se-bearing acanthite, Se-bearing pyrite	
Zapadno-Ozernoe (Belogub et al., 2003; Yakovleva et al., 2003, Ayupova and Tseluyko, 2013, this work)	Native selenium, clausthalite, tiemannite, dzharkenite, naumannite, Se-bearing galena, Se-bearing pyrite, Se tetrahedrite, unidentified As–Sb–Se sulfosalts of Hg and Ag	Se-bearing galena
Yubileynoe (Tatarko, 1996; Vishnevsky et al., 2018, this work)	Clausthalite, tiemannite, naumannite, Se-bearing covellite and chalcocite, Se-bearing chalcopyrite, Se-bearing sphalerite	Se-bearing galena, clausthalite, Se-bearing altaite, Se-bearing ruckligeite
Yuzhno-Kontrolnoe (Belogub, 2009)	Se-bearing tetrahedrite	
Amur (Blinov, 2015)	Clausthalite, tiemannite, naumannite	
Kaban-I (Blinov and Butnyakov, 2016)	Native selenium, clausthalite, naumannite	
Dzhusa (Belogub et al, 2008)	Clausthalite, naumannite, Se-bearing galena	
Molodezhnoe (Ayupova et al., 2015, 2017a,b, this work)		Clausthalite, naumannite, Te-bearing naumannite, bohdanowiczite, Se-bearing galena, Se-bearing roquesite
Letnee (Belogub, 2009)	Se-bearing covellite	
Alexandrinskoe (Ayupova, 2016; Maslennikov et al., 2019)		Se-bearing tetradymite, Se-bearing ruckligeite, Se-bearing tsumoite

from the Gai deposit. At the Zapadno-Ozernoe deposit, the Fe-bearing tiemannite grains < 0.5 μm in size were identified in heavy concentrate of sooty quartz–pyrite sand along with secondary pyrite and dzharkenite (Belogub et al., 2008). At the Yubileynoe deposit, tiemannite was also found in the lower part of oxidation zone.

The Se-bearing sulfides, as well as Se minerals, were found in continental oxidation zones. The Se-bearing acanthite (0.60 wt% Se) was identified in heavy concentrates of native sulfur and quartz sand subzones of the Gai deposit (Zaykov and Sergeev, 1993; Sergeev et al., 1994). The layers of Se-bearing iron disulfides within native sulfur subzone were reported for the Gai deposit (Zaykov and Sergeev, 1993) and Zapadno-Ozernoe deposit, where Se-bearing pyrite form isomorphic series with dzharkenite (Yakovleva et al., 2003). The Se-bearing tetrahedrite (up to 22.84 wt% Se) and unidentified Pb-Ag-Hg sulfosalts (up to 2.27 wt% Se) were described in the lower part of the oxidation zone of the Zapadno-Ozernoye deposit (Belogub et al., 2003).

The Se-bearing rucklidgeite ($PbBi_2Te_4$) was found in the hematite–carbonate gossanites of the Yubileynoe deposit. The Se-bearing rucklidgeite, tsumoite, and tetradymite were also established in gossanites of the Aleksandrinskoe deposit (Ayupova, 2016) (Fig. 8i). These minerals occur at the contacts of partly oxidized chalcopyrite–-sphalerite ore clasts and gangue matrix, in hematite pseudomorphs after ore clasts or in the matrix. Tetradymite contains 0.53–0.66 wt% Se, 0.3–1.07 wt% Ag, and, locally, up to 7.79 wt% Pb. Rucklidgeite contains up to 1.11 wt% Se and up to 2.47 wt% Ag. (Vikentyev et al., 2019).

5.2. Se content and mode of occurrence of Se minerals in the oxidation profiles

Normally, the Se minerals as selenides and native selenium are characteristic of hydrothermal deposits with high Se content, which form at medium or low temperatures (Simon and Essene, 1996; Hannington et al., 1999). The oxidation zones of these deposits, as well as fumaroles, mostly contain selenites rather than selenides (Krivovichev et al., 2011 and reference therein). Finds of selenides in the oxidation zones of the VHMS deposits with initially elevated (but not extreme) Se contents (16–76 ppm, Vikentyev et al., 2019), compared with the average Se contents of the crust as $5*10^{-6}$ (Taylor and McLennan, 1995), look more exotic than ordinary. Only in certain subzones of the continental oxidation zones, such as sulfur sands, the Se content is higher by many orders of magnitude than those of primary massive sulfide ores, which is favorable for the formation of Se minerals. Rare selenides, however, were also found in the upper part of oxidation zones: continental gossans or hematite-enriched gossanites.

Elevated Se contents relative to primary massive sulfide ores is characteristic of the lower leaching (sooty sand) and sulfur subzones of the well-developed continental oxidation zones of the South Urals VHMS deposits. For example, the Se content of a Se-rich darker brown layer among native sulfur zone of the Kul-Yurt-Tau deposit reached 39 wt% (Paley, 1957). The Se content of pyrite–sulfur–quartz sands of the Gai deposit is 0.44 wt% (Zaykov and Sergeev, 1993), which is many times higher than the Se content of primary massive sulfide ores (18–27 ppm; Seravkin and Skuratov, 2009). In the oxidation zone of the Zapadno-Ozernoye deposit, the Se content of sooty quartz sand subzone

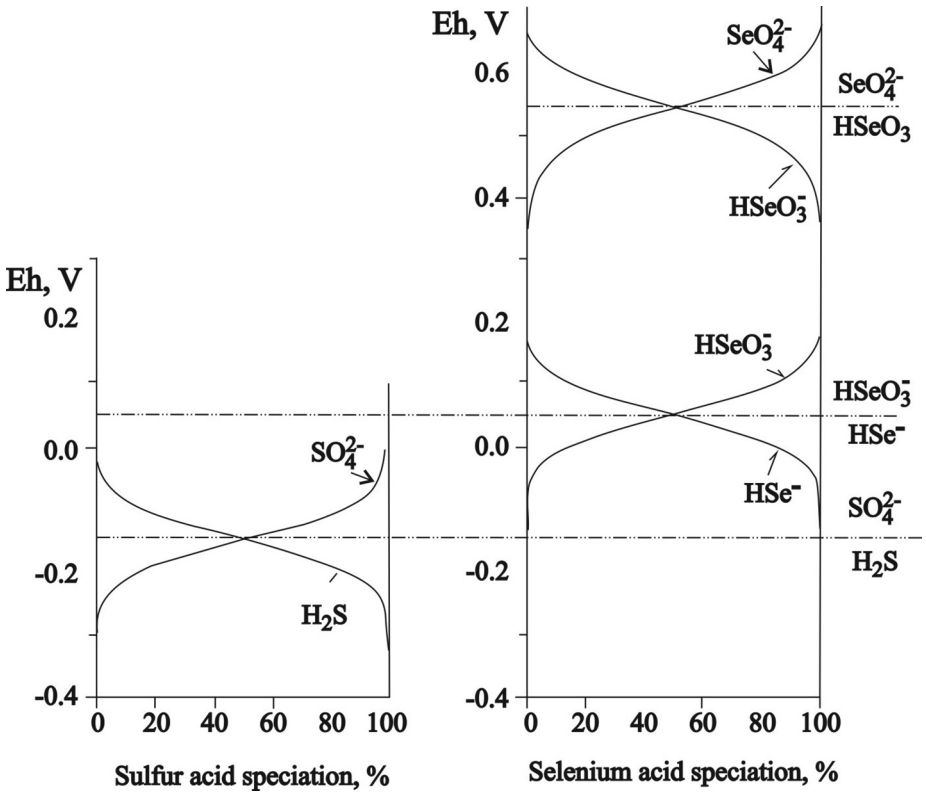

Fig. 11. Distribution of acid-base forms of S and Se acids depending on the Eh of the solution (at 25 °C, 1 bar and pH = 6).

of 311–577 ppm is comparable to the hurricane Se concentrations determined in primary massive sulfide ores. Most Se minerals of the continental oxidation zone have been found in this subzone of these deposits. Selenides of Pb, Ag, and Hg are closely associated with each other and secondary sulfides in the lower part of the continental oxidation zone, which has maximum Se contents. In addition to selenides, native selenium is also found in the thickest oxidation zones with a developed profile containing native sulfur subzone (Table 5).

In the upper part of the leaching subzone (quartz sand) and gossans, the Se content is lower or is similar to that of massive sulfide primary ores. The gossan of Amur deposit contains of 0.2–17 ppm of Se, quartz sand and gossans of Yubileynoe deposit contains of 8 and 120 ppm of Se respectively. Only sporadic selenides or Se-rich secondary sulfides, however, have been found in gossans of the Amur deposit and Yubileynoe deposits, where they are associated with Fe oxyhydroxides and/or Fe carbonates and form individual grains.

No representative data on Se content of various subzones of submarine oxidation zones of the South Urals VHMS deposits are known because of difficult sampling of individual subzones for chemical analysis, since the subzones represent finely intercalated layers penetrating to each other. Nevertheless, according to the available data, the Se content of the products of submarine oxidation is similar or exceeds the Se content of primary massive sulfide ores. In gossanites of the Molodezhnoe deposit, the Se content can be five times higher than that of primary massive sulfide ores: max 1352 ppm Se vs. 30–252 ppm Se, respectively. The Se content of gossanites of the Yubileynoye deposit is similar to that of primary massive sulfide ores and is lower than that of the continental oxidation products.

Thus, the Se minerals have been found in samples from submarine oxidation zones both with elevated and ordinary Se contents and associate with secondary chalcopyrite and Fe oxides (magnetite or hematite). In contrast, no Se minerals have been identified in high-temperature mineral assemblages of hydrothermal smoker chimneys with high Se content, where Se isomorphically substitutes S in chalcopyrite, pyrite and galena (Maslennikov et al., 2014). From thermodynamic viewpoint, however, clausthalite and even native selenium can form in black smoker chimneys associated with peridotites, basalts or sediments under a high rock/water ratio during late low-temperature stages (Tret'yakov and Maslennikov, 2017).

Broadly speaking, selenides in both the continental and submarine oxidation zones formed in similar geological setting. They mostly occur in the lower part of both oxidation zones and are associated with each other and with secondary sulfides. In contrast, in the upper parts of the oxidation zones, they associate with iron oxyhydroxides or oxides. Thus, the finds of Se minerals in submarine and continental oxidation zones of the South Urals VHMS deposits have no direct correlation with bulk Se content of primary or secondary ores. The greatest diversity of Se minerals, however, is typical of native sulfur subzone of the continental oxidation zone with highest Se content.

5.3. Physico-chemical formation conditions of Se minerals and role of bacteria

Empirical data indicate that the Se behavior is redox-controlled, which was demonstrated for roll-front type uranium deposits in sandstones (Simon and Essene, 1996; Shepherd et al., 2005; Spinks et al., 2016, and reference therein). The occurrence of selenides in the continental oxidation zones typically corresponds to the redox barrier as well (Paley, 1957; Belogub et al., 2008). The finding of selenides and Se-bearing chalcopyrite in the Se-depleted gossans, however, requires additional explanation.

In general, selenides form under low temperatures. According to experimental and modeling works, the stability area of selenides expands with decreasing temperature (Simon and Essene, 1996; Akinfiev and Tagirov, 2006). On the basis of thermodynamic calculations, it has been shown that some most common selenides can form under sufficiently high Eh values that is higher than the hematite–magnetite buffer (Simon and Essene, 1996; Charykova et al., 2011). Under low-temperature conditions, the stability field of selenides is shifted to the higher Eh values in comparison with relevant sulfides (Simon and

Essene, 1996; Belogub et al., 2008; Zhu et al., 2012). Moreover, at low temperatures, lower Se activity is required for formation of selenides relative to the S activity required to form appropriate sulfides (Belogub et al., 2008; Vishnevsky et al., 2018). This can be explained by the fact that the reduced forms of Se acids are more stable at higher values of Eh than the corresponding forms of S acids. This is confirmed by changing ratios of various Se and S speciations at variable Eh values and constant pH values. For example, Fig. 11 shows the relative fractions of S and Se dissolved species depending on Eh environment at pH value of 6. It can be seen that the HSe^- is stable at positive Eh value where SO_4^{2-} is stable form of sulfur.

The details of oxidation process vary widely depending on the mineralogy of primary massive sulfide ores, climatic and other factors, and, in particular, the composition of the host rocks. The mineral assemblages and the mineralization sequence of both continental and submarine oxidation zones of the South Urals VHMS deposits may be outlined to provide a background, against which the Eh and pH relations and their control over the distribution of the Se may be discussed.

The Pb, Ag and Hg selenides and native selenium are among the earliest secondary minerals of the oxidation zones of the South Urals VHMS deposits and are mainly developed in the lower part of the oxidation zone at/near the boundary with primary massive sulfide zone. The available values of standard thermodynamic functions of the formation of some selenides have previously been summarized and the Eh–pH diagrams of the Me–S–Se–H_2O systems (Me = Fe, Pb, Ag, Hg) have been calculated (Vishnevsky et al., 2018). In this paper, the stability fields for Pb, Hg and Ag selenides and co-existing Fe phases are plotted on Eh–pH diagrams (Fig. 12a–c) to characterize the physicochemical conditions of stability of brown ore minerals (goethite/hematite and siderite) and newly formed Hg (tiemannite), Ag (naumannite), and Pb (clausthalite) selenides.

The Fe oxyhydroxides or oxides, siderite and barite are key mineral assemblages in both continental and submarine oxidation zones of the South Urals VHMS deposits (Table 6), thus, they were used to constrain Eh and pH values of formation of most common selenides (Fig. 12). The precipitation of barite upon sulfide oxidation indicates that the solutions evolved to higher O fugacity (i.e., sulfate-stable) and/or higher $a_{Ba^{2+}}$. The presence of Fe oxyhydroxides/oxides in oxidation zones was also consistent with higher O fugacity conditions.

The idealized Eh–pH relations in the continental oxidized zone of the South Urals VHMS deposits based on the foregoing discussion are indicated in Fig. 12. These relations are primarily correlated with the access of oxygen. Assuming access of oxygen from the surface, the minimal concentration of oxygen is reached at the interface with the sulfide zone. Below this level, which ideally coincides with the water table, the environment become reducing with wide range of pH.

The initial formation conditions of the submarine oxidation zone are weakly alkaline (under standard conditions, the pH value of seawater is 7.85–8.15) and oxidative (Eh ~ 0.7 V with a tendency to increase with decreasing temperature) (Steele et al., 2010). The pH values of pore solution changes to more acidic and reducing because of the interaction between seawater and primary sulfides (Hannington et al., 1999).

The chemistry of oxidation of primary Se-bearing sulfides indicates that secondary selenides of the South Urals VHMS deposits formed under neutral or slightly acid conditions (pH 5.5–6.5) with a positive or close to Eh value of 0 (as indicated by the position of the siderite stability field).

Clausthalite (PbSe) forms as a secondary mineral of the oxidation zones, typically, by oxidation of galena and pyrite. In Eh–pH diagram of the Pb–Fe–Se–S–CO_2–H_2O system (Fig. 12a), the intermediate part is occupied by stability field of clausthalite, which is stable in the stability field of native selenium. At low Eh vlaues, Pb occurs in form of Se-bearing galena, which can be oxidized with the increasing Eh values and subsequent formation of clausthalite:

$$Pb(S_{1-x}Se_x) + (4 - 4x)H_2O = Pb^{2+} + (1 - x)SO_4^{2-} + xHSe^- + (8 - 7x)H^+ + (8 - 8x)e, \quad (1)$$

$$Pb^{2+} + HSe^- = PbSe + H^+. \quad (2)$$

The anion SO_4^{2-}released during reaction (1) can also react with Ba^{2+} to form barite:

$$Ba^{2+} + SO_4^{2-} = BaSO_4. \quad (3)$$

The Se-bearing pyrite from primary massive sulfide ores is also oxidized in leaching and gossan subzones, but Fe selenides (dzharkenite, $FeSe_2$, and achavalite, FeSe) are unstable there, since Fe is oxidized with the formation of goethite and dissolved selenium-bearing ion:

$$FeSe_2 + 8H_2O = FeO(OH) + 2HSeO_3^- + 13H^+ + 13e \quad (4)$$

$$FeSe + 5H_2O = FeO(OH) + HSeO_3^- + 8H^+ + 7e \quad (5)$$

In more oxidizing conditions, clausthalite is unstable and is

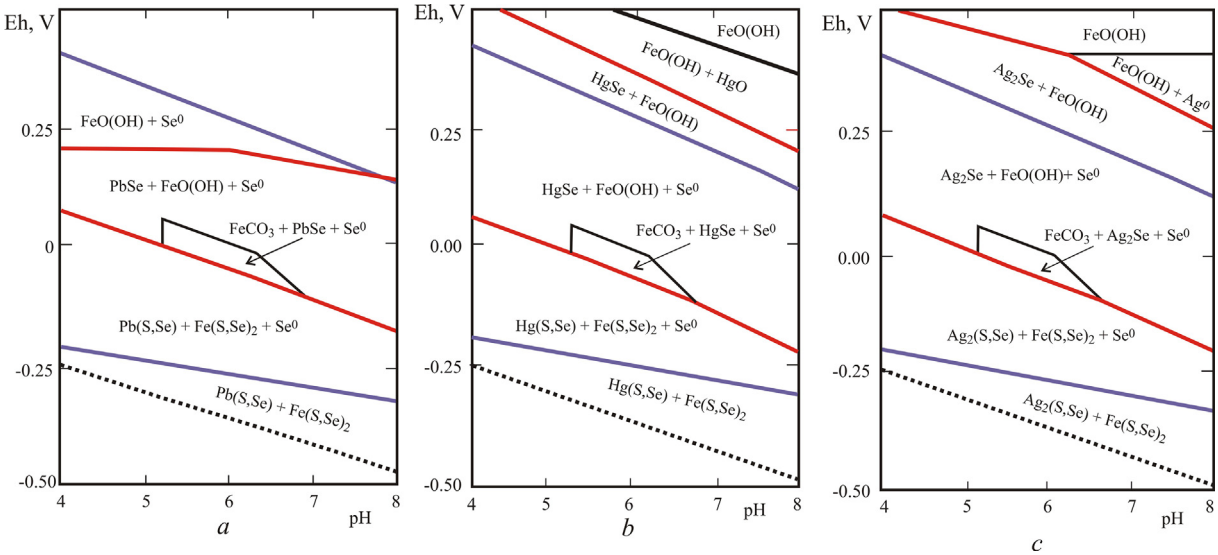

Fig. 12. Eh–pH diagrams of the systems: (a) Pb-Fe-S-Se-CO_2–H_2O; (b) Hg-Fe-Se-S-CO_2-H_2O; (c) Pb-Fe-S-Se-CO_2-H_2O at 25 °C and 1 bar pressure. *Abbreviations*: Stability fields of native selenium (blue solid lines) and selenides (red solid lines). (For interpretation of the references to colour in this figure legend, the reader is referred to the web version of this article.)

Table 6
Key minerals of the continental and submarine oxidation zones.

Subzone	Continental	Submarine
Iron cap (gossan)	Goethite, hematite, siderite*, base metal salts of oxygen acids	Hematite, quartz, chlorite, carbonates (calcite, Mn calcite, ankerite, monheimite, siderite)
Jarosite	Jarosite supergroup minerals (jarosite, beudantite, alunite), kaolinite, illite	–
Leaching	Quartz, barite, pyrite, anglesite, silver halogenides	Quartz, barite, pyrite
Native sulfur	Native sulfur	–
Secondary enrichment (supergene sulfide)	Chalcocite group minerals, covellite	Chalcopyrite, sphalerite, tennantite, bornite

Note. Dash, no jarosite and native sulfur subzones are present in the submarine oxidation zone. * – only Yubileynoe deposit.

decomposed with the formation of dissolved particles:

$$PbSe + 3H_2O = Pb^{2+} + HSeO_3^- + 5H^+ + 6e \quad (6)$$

or

$$PbSe + 4H_2O = PbOH^+ + HSeO_3^- + 6H^+ + 6e. \quad (7)$$

The stability fields of tiemannite (HgSe) and naumannite (Ag_2Se) are likely similar to those of claustalite (PbSe) (Fig. 12b and c). Tiemannite and naumannite are oxidized to native mercury and native silver following reactions (8) and (9), respectively:

$$HgSe + 3H_2O = Hg^0 + HSeO_3^- + 5H^+ + 4e. \quad (8)$$

$$Ag_2Se + 3H_2O = 2Ag^0 + HSeO_3^- + 5H^+ + 4e. \quad (9)$$

Thus, if the Se activity is sufficient for the formation of selenides, they can associate with Fe^{3+} minerals (hematite or goethite). Such associations have been described at Corvusine (Utah), Rifle and Garfield (Colorado) roll-front type uranium deposits (Simon et al., 1997).Spinks et al. (2016) showed that selenide crystallization can be triggered by a subtle shift of Eh values, which can be related to the bacterial activity. The Fe(III)-reducing bacteria may concentrate Se on the surface of Fe(III) oxides, on the particles of which they can form coatings (Klonowska et al., 2005; Pearce et al., 2009). These bacteria can build local reduced zones on the oxide surface, which are favorable for Se accumulation. It should be noted, that bacterial influence on the formation of native selenium is rather possible, since a number of anaerobic Se bacteria are known today. These bacteria extract selenite ion from the media and synthesize intracellular inclusions of native selenium (Borghese et al., 2014). Selenite-reductive bacteria, isolated from Se-bearing agriculture soils of India, supported synthesis of extracellular native selenium (Bajaj and Winter, 2014). Similar bacteria may occur in the oxidation zones and may be the reason for crystallization of selenides even at low Se content of supergene solutions. This is in line with accumulation of Se by organic matter upon atmospheric oxidation of sulfide ores in the Kisgruva mine region (Norway) (Bullock et al., 2018).

Presence of thio- and iron bacteria in the oxidation zones is commonly accepted (Yakhontova and Grudnev, 1987). For the oxidation zones of the Zapadno-Ozernoe and Blyava VHMS deposits in the South Urals, the role of bacteria in the formation of secondary chalcogenides was supported by their extremely low S isotopic composition (δS^{34} up to –17.2‰) (Belogub et al., 2008). At the Yubileynoe deposit, the secondary Se-bearing chalcopyrite is associated with siderite exhibiting very low C isotopic composition ($\delta^{13}C$ = from –20.0 to –23.4‰ PDB), which corresponds to that of the fermented wood relics in the overlapping sediments (Novoselov et al., 2019). These facts indirectly point to the involvement of bacteria in the formation of the continental oxidation zones. Numerous bacterial relics were found in the submarine oxidation zones as well (Ayupova and Maslennikov, 2013; Ayupova et al., 2017b). Thus, the sporadic presence of selenides in assemblage with Fe(III) oxides/oxyhydroxides could reflect a bacterial-induced redox barrier. The formation of selenides is controlled by the ratio of Se and S activities. The formation of specific selenides depends on the metal activity ratios.

5.4. Source of Se

The main source of Se for supergene chalcogenides of the oxidation zones of the South Urals VHMS deposits is related to primary massive sulfide ores with high-temperature Se-bearing chalcopyrite. Colloform pyrite with high concentration of trace elements could also be a source of Se, as well as of Pb, Ag and Hg, for secondary selenides because of the release of incoherent metals and Se during diagenesis (Auclair et al., 1987; Maslennikov et al., 2014, 2017). Decomposition of these sulfides under oxidizing conditions can lead to precipitation of selenides.

The submarine oxidation zones of the VHMS deposits start to form during the life cycle of the seafloor hydrothermal system. Thus, additional Se source is related to the hydrothermal fluid. In the present-day and ancient seafloor volcanic-dominated hydrothermal systems, Se may derive from seawater or leaching of igneous rocks and/or magma degassing. Seawater is typically characterized by low Se content (170 ng/kg), which occur as dissolved Se^{VI}, Se^{IV} and Se^{-II} species or as organic-incorporated Se depending on the redox conditions (Measures and Burton, 1980). In anoxic basins, the bottom waters and associated anoxic sediments have elevated Se contents (Kluckhohn et al., 1990; Mercone et al., 1999). The higher Se contents are controlled by Se reduction in an anoxic water column and below the seawater–sediment surface. Magmatic sources, such as shallow-seated magmas and their derivative rocks of the VHMS systems, have low Se contents (< 2 ppm), which, nevertheless, may contribute Se via hydrothermal fluid leaching or via contemporaneous magma degassing, assuming a Se behavior similar to that of sulfur (e.g., de Ronde et al., 2005).

6. Concluding remarks

The selenides and Se-bearing chalcogenides of the South Urals VHMS deposits are found in the low-temperature mineral assemblages of the continental and submarine oxidation zones. The Se minerals are more characteristic of the lower part of the continental oxidation zone: secondary copper enrichment and the bottom of leaching and sulfur subzones. The Se minerals also occur in the continental gossans and submarine gossanites. In assemblage with Fe(III) oxides/oxyhydroxides, selenides and Se-bearing sulfides can be a result of low S activity, when Se can successfully compete with S for the formation of the chalcogenides. The formation of selenides in the upper parts of both oxidation zones is related to the local redox barrier, which possibly forms due to vital functions of living organisms.

Declaration of Competing Interest

The authors declare that they have no known competing financial interests or personal relationships that could have appeared to influence the work reported in this paper.

Acknowledgements

The field works at the VHMS deposits of the South Urals were supported by the Russian Science Foundation, project no. 14-17-00691. The mineralogical and analytical studies were supported by State Contract of the SU FSC MG UB RAS no. AAAA-A19-119061790049-3. We thank Marina Malyarenok and Kseniya Filippova for analytical works, Irina Melekestseva for help in preparation of the manuscript and anonymous reviewers for useful comments.

Appendix A. Supplementary data

Supplementary data to this article can be found online at https://doi.org/10.1016/j.oregeorev.2020.103500.

References

Akinfiev, N.N., Tagirov, B.R., 2006. Effect of Se on silver transport and precipitation by hydrothermal solutions: thermodynamic description of the Ag–Se–S–Cl–O–H system. Geol. Ore Dep. 48 (5), 402–424.

Auclair, G., Fouquet, Y., Bohn, M., 1987. Distribution of Se in high-temperature hydrothermal sulfide deposits at 13N East Pacific Rise. Can. Mineral. 25, 577–588.

Ayupova, N.R., Maslennikov, V.V., 2013. Biomorphic textures in the ferruginous–siliceous rocks of massive sulfide bearing paleohydrothermal fields in the Urals. Lithol. Miner. Resour. 48, 438–455.

Ayupova, N.R., Tseluyko A.S., 2013. Sulfide-magnetite ores from Zapadno-Ozernoe copper-zink massive sulfide deposit (Southern Urals). Metallogeny of ancient and modern oceans-2013. Miass, Institute of Mineralogy UB RAS. P. 139–143 (in Russian).

Ayupova, N.R., Maslennikov, V.V., Maslennikova, S.P., Blinov, I.A., Danyushevsky, L.V., Large, R.R., 2015. Rare mineral and trace element assemblages in submarine supergene zone at the Devonian Molodezhnoye VMS deposit, the Urals, Russia. Proceedings of the 13 SGA Biennial Meeting. Nancy, 4, pp. 1512–1515.

Ayupova, N.R., 2016. Bi–minerals in gossanites of Alexandrinskoe copper-zink massive sulfide deposit (Southern Urals). Proccedings of the 68 South Urals State Universitaty conference, pp. 261–264.

Ayupova, N.R., Maslennikov, V.V., Kotlyarov, V.A., Maslennikova, S.P., Danyushevsky, L.V., Large, R., 2017a. Se and In minerals of the submarine oxidation zone of a massive sulfide orebody of the Molodezhnoe copper-zink massive sulfide deposit, Southern Urals. Doklady Earth Sci. 473, 318–322.

Ayupova, N.R., Maslennikov, V.V., Tessalina, S.G., Shilovsky, O.P., Sadykov, S.A., Hollis, S.P., Danyushevsky, L.V., Safina, N.P., Statsenko, E.O., 2017b. Tube fossils from gossanites of the Urals VMS deposits, Russia: authigenic mineral assemblages and trace element distributions. Ore Geol. Rev. 85, 107–130.

Ayupova, N.R., Melekestseva, I.Yu., Maslennikov, V.V., Tseluyko, A.S., Blinov, I.A., Beltenev, V.E., 2018. Uranium accumulation in modern and ancient Fe-oxide sediments: examples from the Ashadze-2 hydrothermal sulfide field (Mid-Atlantic Ridge) and Yubileynoe massive sulfide deposit (South Urals, Russia). Sediment. Geol. 367, 164–174.

Bajaj, M., Winter, J., 2014. Se (IV) triggers faster Te (IV) reduction by soil isolates of heterotrophic aerobic bacteria: formation of extracellular SeTe nanospheres. Microb. Cell Fact. 13, 168. https://doi.org/10.1186/s12934-014-0168-2.

Belogub, E.V. Supergenesis of the sulfide deposits of the South Urals, 2009. Thesis of doctoral dissertation. Miass (in Russian).

Belogub, E.V., Novoselov, C.A., Spiro, B., Yakovleva, B., 2003. Mineralogical and sulphur isotopic features of the supergene profile of Zapadno-Ozernoye massive sulphide and gold-bearing gossan deposit, South Urals. Mineral. Mag. 67, 339–354.

Belogub, E.V., Novoselov, K.A., Yakovleva, V.A., Spiro, B., 2008. Supergene sulphides and related minerals in the supergene profiles of VMS deposits from the South Urals. Ore Geol. Rev. 33, 239–254.

Bethke, C.M., Yeakel, S., 2011. The Geochemist's Workbench, Release 9.0, GWB Essentials Guide. Aqueous Solutions, LLC, University of Illinois, Champaign.

Blinov, I.A., 2015. Native metals, selenides, halides and associated minerals of limonite ores from the Amur and Verhne Arshinsky deposit (Southern Urals). Litosfera 1, 65–74 (in Russian).

Blinov, I.A., Butnyakov, A.V., 2016. Minerals of oxidation zone of Kaban massive sulfide deposit (Middle Urals). Metallogeny of ancient and modern oceans-2016. Miass, Institute of Mineralogy UB RAS, pp. 70–74 (in Russian).

Borghese, R., Baccolini, C., Francia, F., Sabatino, P., Turner, R.J., Zannoni, D., 2014. Reduction of chalcogen oxyanions and generation of nanoprecipitates by the photosynthetic bacterium Rhodobacter capsulatus. J. Hazard. Mater. 269, 24–30.

Brodtkorb, M.K., Paar, W.H., 1993. New data on the ore mineralogy of the Upulungos mine, La Mejicana district, Sierra de Famatina, Argentina. In: Fenoll, P., Hach, A.F., Torres-Ruiz, J., Gervilla, F. (Eds.), Current Research in Geology Applied to Ore Deposits Proceedings 2nd Biennial Soc. Geol. Applied to Mineral Deposits Meeting, Granada, Spain, pp. 57–59.

Bullock, L., Perez, M., Armstrong, J., Parnell, J., Still, J., Feldmann, J., 2018. Selenium and tellurium resources in Kisgruva Proterozoic volcanogenic massive sulphide deposit (Norway). Ore Geol. Rev. 99, 411–424.

Charykova, M., Krivovichev, V., Depmeier, W., 2011. Thermodynamics of arsenates, selenites, and sulfates in the oxidation zone of sulfide ores. II. Systems M_1, M_2^0// SO_4^{2-}–H_2O (M_1, M_2^0 = Fe^{2+}, Fe^{3+}, Cu^{2+}, Zn^{2+}, Pb^{2+}, Ni^{2+}, Co^{2+}, H^+) at 25 °C. Geol. Ore Dep. 52, 701–780.

Ciobanu, C., Cook, N., Spry, P., 2006. Preface – Special issue: telluride and selenide minerals in gold deposits – How and why? Miner. Petrol. 87, 163–169.

Cook, D.R., McPhai, I.D.C., 2001. Epithermal Au-Ag-Te mineralization, Acupan, Baguio Philippines; numerical simulations of mineral deposition. Econ. Geol. 96, 109–131.

de Ronde, C.E.J., Hannington, M.D., Stoffers, P., Wright, I.C., Ditchburn, R.G., Reyes, A.G., Baker, E.T., Massoth, G.J., Lupton, J.E., Walker, S.L., Greene, R.R., Soong, C.W.R., Ishibashi, J., Lebon, G.T., Bray, C.J., Resing, J.A., 2005. Evolution of a submarine magmatic-hydrothermal system: Brothers volcano, southern Kermadec arc, New Zealand. Econ. Geol. 100, 1097–1133.

Holland, H.D., Turekian, K.K. (Eds.), 2005. Environmental Geochemistry. Elsevier, Amsterdam-Tokyo.

Finkelman, R.B., 1985. Mode of occurrence of accessory sulfide and selenide minerals in coal. Compte Rendu, Neuvième Congrès International de Stratigraphie et de Géologie du Carbonifère 4, 407–412.

Förster, H.-J., Tischendorf, G., Rhede, D., 2005. Mineralogy of the Niederschlema-Alberoda U-Se–polymetallic deposit, Erzgebirge, Germany. V. Watkinsonite, nevskite, bohdanowiczite and other bismuth minerals. Can. Miner. 43, 899–908.

Gavrilov, V.A., Skuratov, V.N., Ismagilov, M.I., 1984. Structure and conditions of localization of the Zapadno-Ozernoye massive sulfide deposit. Doklady Acad. Sci. USSR 1, 161–164.

Hannington, M.D., Herzig, P.M., Scott, P., Thompson, G., Rona, P.A., 1991. Comparative mineralogy and geochemistry of gold-bearing sulphide deposits on the Mid Ocean Ridges. Mar. Geol. 101, 217–248.

Hannington, M.D., Bleeker, W., Kjarsgaard, I., 1999. Sulfide mineralogy, geochemistry, and ore genesis of the Kidd Creek Deposit: Part II. The bornite zone. Econ. Geol. Monogr. 10, 225–266.

Hannington, M.D., Thompson, G., Rona, P.A., Scott, S.D., 1988. Gold and native copper in supergene sulphides from the Mid-Atlantic Ridge. Nature 333 (6168), 64–66.

Herrington, R., Zaykov, V., Maslennikov, V., Brown, D., Puchkov, V., 2005. Mineral deposits of the Urals and links to geodynamic evolution. Econ. Geol. One Hundredth Anniv 1069–1095.

Herzig, P.M., Hannington, M.D., Scott, S.D., Maliotis, G., Rona, P.A., Thompson, G., 1991. Gold-rich sea-floor gossans in the Troodos ophiolite and on the Mid-Atlantic Ridge. Econ. Geol. 86, 1747–1755.

Huston, D.L., Sie, S.H., Suter, G.F., Cooke, D.R., Both, R.A., 1995. Trace elements in sulfide minerals from eastern Australian volcanic-hosted massive sulfide deposits; Part I, Proton microprobe analyses of pyrite, chalcopyrite, and sphalerite, and Part II, Se levels in pyrite; comparison with delta (super 34) S values and implications for the source of sulfur in volcanogenic hydrothermal systems. Econ. Geol. 90, 1167–1196.

Jonsson, E., Wagner, T., 2002. Ore mineralogy of the Skrikerum Cu-Ag-Tl-(Au) selenide deposit, SE Sweden: preliminary results. In: Jónsson, S.S. (Ed.), 25th Nordic Geological Winter Meeting, Reykjavík, Abstract vol. 98.

Klonowska, A., Heulin, T., Vermeglio, A., 2005. Selenite and tellurite reduction by Shevanella oneidensis. Appl. Environ. Microbiol. 71, 5607–5609.

Kluckhohn, R.S., Cutter, G.A., Radford-Knoery, J., 1990. Se and sulfur in Black Sea sediments. EOS Trans. Am. Geophys. Union 71, 151.

Krivovichev, V.G., Charykova, M.V., Yakovenko, O.S., Depmeier, W., 2011. Thermodynamics of arsenates, selenites, and sulphates in oxidizing zone of sulphide ores. IV. Eh–pH graphs for system Me–Se–H_2O systems (Me = Co, Ni, Fe, Cu, Zn, Pb) at 25 °C. Geol. Ore Dep. 53, 514–527.

Krivovichev, V.G., Charykova, M.V., 2006. Thermodynamics of mineral equilibria in the system with toxic components 1. Se: tutorial and handbook. Saint-Petersburg: SOLO (in Russian).

Krivovichev, V.G., Charykova, M.V., Vishnevsky, A.V., 2017. The thermodynamics of selenium minerals in near-surface environments. Minerals 7 (10), 188.

Layton-Matthews, D., Leybourne, M.I., Peter, J.M., Scott, S.D., Cousens, B., Eglington, B., 2013. Multiple sources of Se in ancient seafloor hydrothermal systems: compositional and Se, S and Pb isotopic evidence from volcanic-hosted and volcanic-sediment-hosted massive sulfide deposits of the Finlayson Lake district, Yukon, Canada. Geochim. Cosmochim. Acta 117, 313–331.

Maslennikov, V.V., Ayupova, N.R., Safina, N.P., Tseluyko, A.S., Melekestseva, I.Yu., Large, R.R., Herrington, R.J., Kotlyarov, V.A., Blinov, I.A., Maslennikova, S.P., Tessalina, S.G., 2019. Mineralogical features of ore diagenites in the Urals massive sulfide deposits, Russia. Minerals 9 (150). https://doi.org/10.3390/min9030150.

Maslennikov, V.V., Ayupova, N.R., Herrington, R.J., Danyushevskiy, L.V., Large, R.R., 2012. Ferruginous and manganiferous haloes around massive sulphide deposits of the Urals. Ore Geol. Rev. 47, 5–41.

Maslennikov, V.V., Ayupova, N.R., Maslennikova, S.P., Tret'yakov, G.A., Danyushevsky, L.V., Large, R.R., Melekestseva, I. Yu., Safina, N.P., Belogub, E.V., Tseluyko, A.S., Gladkov, A.G., Kraynev, Yu.D., 2014. Toxic elements in massive sulfide forming systems. UB RAS, Yekaterinburg (in Russian).

Maslennikov, V.V., Ayupova, N.R., Maslennikova, S.P., Tseluyko, A.S., Large, R., Danyushevsky, L.E., Lein, A.Yu., Bogdanov, Yu.A., 2013. Mineral and chemical peculiarities of vent chimneys from the Yubileynoye VMS deposit at the Early Devonian basalt-boninite basement of West Magnitogorsk arc, the Southern Urals, Russia. Proceedings of the 12 SGA Biennial Meeting. Uppsala, 4, pp. 1512–1515.

Maslennikov, V.V., Maslennikova, S.P., Large, R.R., Danyushevsky, L.V., Herrington, R.J., Ayupova, N.R., Zaykov, V.V., Lein, A.Yu., Tseluyko, A.S., Melekestseva, I.Yu., Tessalina, S.G., 2017. Chimneys in Paleozoic massive sulfide mounds of the Urals VMS deposits: mineral and trace element comparison with modern black, gray and clear smokers. Ore Geol. Rev. 85, 64–106.

Measures, C.I., Burton, J.D., 1980. The vertical distribution and oxidation states of dissolved Se in the northeast Atlantic Ocean and their relationship to biological

processes. Earth Planet. Sci. Let. 46 (3), 385–396.
Mercone, D., Thomson, J., Croudace, W., Troelstra, S.R., 1999. A coupled natural immobilization mechanism for mercury and Se in deep-sea sediments. Geochim. Cosmochim. Acta 63, 1481–1488.
Yushkin, N.P. (Ed.), 1991. Mineralogy of Urals, Sverdlovsk: UB RAS (in Russian).
Novoselov, K.A., Belogub, E.V., Sadykov, S.A., Vikentyev, I.V., 2019. Gossan of the Yubileynoe massive sulfide deposit (South Urals): evidence for formation on the seafloor. Lithol. Miner. Resour. 54 (1), 66–78.
Paley, I., 1957. Native Se concentration in the oxidation zone in a sulphide deposit. Geokhimiya 7, 640–641 (in Russian).
Pearce, C.I., Pattrick, R.A.D., Law, N., Charnock, J.M., Coker, V.S., Fellowes, J.W., Oremland, R.S., Lloyd, J.R., 2009. Investigating different mechanisms for biogenic selenite transformations: *Geobacter* sulfurreducens, Shewanella oneidensis and Velionella atypica. Environ. Technol. 30, 1313–1326.
Poluektov T., A., Erkomov I., V., Milashich I., A., Ponomareva P., R., 1974. Report about geological exploration of the Letnee copper massive sulfide deposit at the Southern Urals (in Russian). Orenburggeologia.
Prokin, V.A., Buslaev, F.P., 1999. Massive copper-zinc sulphide deposits in the Urals. Ore Geol. Rev. 14, 1–69.
Puchkov, V.N., 2017. General features relating to the occurrence of mineral deposits in the Urals: What, where, when and why. Ore Geol. Rev. 85, 4–29.
Ryser, A.L., Strawn, D.G., Marcus, M.A., Johnson-Maynard, J.L., Gunter, M.E., Möller, G., 2005. Micro-spectroscopic investigation of Se-bearing minerals from the Western US Phosphate Resource Area. Geochem. Trans. 6 (1), 1–11.
Seravkin, I.B., 2010. The metallogeny of the South Urals and Central Kazakhstan. Gilem, Ufa (in Russian).
Seravkin, I.B., Skuratov, B.N., 2009. Gai copper massive sulfide deposit: structure, zoning and distribution of gold and silver. Lithosphere 4, 66–72 (in Russian).
Seravkin, I.B., Snachev, V.I., 2012. Stratiform base-metal deposits in the eastern province of the Southern Urals, Russia. Geol. Ore Dep. 54 (3), 209–218.
Sergeev, N., Zaykov, V., Laputina, I., Trofimov, O., 1994. Gold and silver in the supergene zone of Gai sulphide deposit (S. Urals). Geol. Rudn. Mestorozh. 36 (2), 169–183 (in Russian).
Shepherd, T.J., Bouch, J.E., Gunn, A.G., McKervey, J.A., Naden, J., Scrivener, R.C., Styles, M.T., Large, D.E., 2005. Permo-Triassic unconformity-related Au-Pd mineralization, South Devon, UK: new insights and the European perspectives. Miner. Dep. 40, 24–44.
Simon, G., Essene, E., 1996. Phase relations among selenides, sulfides, tellurides and oxides: I. Thermodynamic properties and calculated equilibria. Econ. Geol. 91, 1183–1208.
Simon, G., Kesler, H., Essene, E., 1997. Phase relations among selenides, sulfides, tellurides, and oxides: II. Applications to selenide-bearing ore deposits. Econ. Geol. 92 (4), 468–484.
Spinks, S.C., Parnell, J., Bellis, D., Still, J., 2016. Remobilization and mineralization of Se-tellurium in metamorphosed red beds: evidence from the Munster Basin, Ireland. Ore Geol. Rev. 72, 114–127.
Steele, J.H., Thorpe, S.A., Turekian, K.K., 2010. Marine Chemistry and Geochemistry: A Derivative of Encyclopedia of Ocean Sciences, second ed. Elsiever, London.
Tatarko N.I., 1996. Gossans lodes of Yubileynoe deposit. Report about preliminary prospection with reserve calculation as of 01.12.1996. Sibay (in Russian).
Taylor, S.R., McLennan, S.M., 1995. The geochemical evolution of the continental crust. Rev. Geophys. 33, 241–265.
Tret'yakov, G.A., Maslennikov, V.V., 2017. Comparison of mineral assemblages in various smokers: data on paragenetic analysis and physico-chemical modeling. Mineralogy 3 (1), 71–81 (In Russian).
Tseluyko, A.S., Maslennikov, V.V., Ayupova, N.R., Maslennikova, S.P., Danyushevsky, L.V., 2019. Tellurium-bearing minerals in clastic ores of Yubileynoe massive sulfide deposit (South Ural). Geol. Ore Dep. 2, 134–162.
Vikentyev, I.V., Belogub, E.V., Moloshag, V.P., 2019. Selenium in massive sulfides. Doklady Earth Sci. 43 (3), 67–70.
Vikentyev, I.V., Belogub, E.V., Novoselov, K.A., Moloshag, V.P., 2017. Metamorphism of volcanogenic massive sulphide deposits in the Urals. Ore geology. Ore Geol. Rev. 85, 30–63.
Vishnevsky, A.V., Belogub, E.V., Charykova, M.V., Krivovichev, V.G., Blinov, I.A., 2018. Thermodynamics of arsenates, selenites, and sulfates in the oxidation zone of sulfide ores. XIV. Se minerals in the oxidation zone of the Yubileynoe massive sulfide deposit, the South Urals. Geol. Ore Dep. 60 (7), 559–567.
Wagner, T., Jonsson, E., 2001. Mineralogy of sulfosalt-rich vein-type ores, Boliden massive sulfide deposit, Skellefte destrict, Northern Sweden. Can. Miner. 39, 855–872.
Willgallis, A., Özgür, N., Siegmann, E., 1990. Se- and Te-bearing sulphides in copper ore deposits of Murgul, NE Turkey. Eur. J. Miner. 2, 145–148.
Yakhontova, L.K., Grudnev, A.P., 1987. Mineralogy of Oxidized Ores. Handbook. Moscow: Nedra (in Russian).
Yakovleva, V.A., Belogub, E.V., Novoselov, C.A., 2003. Supergene iron sulphoselenides from Zapadno-Ozernoe copper-zinc massive sulphide deposit, South Urals: the new solid solution series between pyrite FeS_2 and dzharkenite $FeSe_2$. Miner. Mag. 67 (2), 355–364.
Yushko-Zakharova, O.E., Ivanov, V.V., Vorob'eva, M.S., Dubakina, L.S., Razina, I.S., Karpukhina, V.S., 1978. Geochemistry of Se, Te and Bi in massive sulphide deposits of the Urals and some problems of ore genesis. Geokhimiya 9, 1368–1378 (in Russian).
Zaykov, V.V., Sinakovskaya, I.V., San'ko, L.A., 1987. Pyrite-pyrophyllite Kul-Yurt-Yau deposit, Bashkiria. Geol. Ore Dep. 4, 58–68 (in Russian).
Zaykov, V., Sergeev, N., 1993. Supergenesis zone of the Gai VMS deposit (Southern Urals). Geol. Rudn. Mestorozh. 35, 320–332 (in Russian).
Zaykov, V.V., Maslennikov, V.V., Zaykova, E.V., Herrington, R., 2001. Ore-formational and ore-facies analysis of the massive sulfide deposits of Ural paleo-ocean. Miass: IMin UB of RAS (in Russian).
Zhu, J.-M., Johnson, T.M., Finkelman, R.B., Zheng, B.-S., Sýkorová, I., Pešek, J., 2012. The occurrence and origin of Se minerals in Se-enriched stone coals, spoils and their adjacent soils in Yutangba, China. Chem. Geol. 330–331, 27–38.